Photonic processing of microwave signals

J. Capmany, D. Pastor, B. Ortega, J. Mora and M. Andrés

Abstract: In this paper, recent advances in the implementation of photonic tuneable transversal filters for RF signal processing developed by the Optical Communications Group are described. After a brief introduction to the field and the basic concepts, limiting factors and application of these filters are described in the field. This is based on a distinction between filters based on wavelength tuneable optical taps and others based on the tuneability of the dispersive elements that provide the time delay between samples. Recently developed approaches have also been discussed.

1 Introduction

The impressive development of photonics technology over the last 25 years has paved the way for the implementation of increasingly higher bandwidth digital and analog fibre-optic communication systems. In the later case, it has been the exploitation of the unique properties that photonic devices and systems bring to the generation, transport, processing and detection of radiofrequency, microwave and millimetre-wave signals which has acted as a key enabling technology and rendered a new research area given the name of 'microwave photonics' [1].

Within the field of microwave photonics one of the applications that first attracted the interest of the researchers has been driven by the possibility of using photonic devices to implement flexible filters to carry signal processing functions in radio frequency systems. Considerable research efforts have been carried over this period using different technology alternatives that have been reported in the literature [2–62]. This approach involves the use of photonics technology and especially fibre and integrated photonic devices and circuits to perform the required signal processing tasks over the target RF signals conveyed by an optical carrier directly in the optical domain. Also, in the context of subcarrier multiplexed WDM optical label swapping networks, there is an increasing use of the RF and microwave spectrum together with the baseband portion inside an optical channel to carry simultaneously payload and label information (the payload occupies the baseband region and the header or label is placed on a subcarrier above baseband). Therefore there is a need to access or process both payload and header directly in the optical domain at intermediate nodes in the network for routing purposes. Thus, there are two main driving application fields: (*a*) RF systems and applications and (*b*) optical transmission systems and networks.

In the first field, the traditional approach towards RF signal processing is shown in the upper part of Fig. 1, where the RF signal originated at a RF source or coming from an antenna is fed to a RF circuit that performs the signal processing tasks either at the RF signal or at an intermediate frequency band after a down-conversion operation. In any case, the RF circuit is capable of performing the signal processing tasks for which it has been designed only within a specified (often reduced) spectral band. This approach results in a poor flexibility since changing the band of the signals to be processed requires the design of a novel RF circuit and possibly the use of a different hardware technology. Furthermore, even if the RF carrier is not changed, the nature of the modulating signal might be, requiring more bandwidth or sampling speed from the processor. These limitations are known in the literature as the 'electronic bottleneck' [2].

An interesting approach to overcome the above limitations involves the use of photonics technology and especially fibre and integrated photonic devices and circuits to perform the required signal processing tasks of RF signals conveyed by an optical carrier directly in the optical domain. The discrete-time optical processing of microwave signals (DOPMS) approach is shown in the lower part of Fig. 1. The RF to optical conversion is achieved by direct (or externally) modulating a laser. The RF signal is conveyed by an optical carrier and the composite signal is fed to a photonic circuit that samples the signal in the time domain, weights the samples and combines them using optical delay lines and other photonic elements. At the output(s) the resulting signal(s) are optically to RF converted by means of an/various optical receiver(s). The use of this photonic approach brings considerable potential advantages:

1. Optical delay lines have very low loss (independent of the RF signal frequency).
2. Provide very high time bandwidth products.
3. Are immune to electromagnetic interference (EMI).
4. Are lightweight.
5. Can provide very short delays which result in very high speed sampling frequencies (over 100 GHz in comparison with a few GHz with the available electronic technology).

IEE Proceedings online no. 20050018

doi:10.1049/ip-opt:20050018

Paper first received 10th February and in final revised form 27th July 2005

J. Capmany, D. Pastor, B. Ortega and J. Mora are with Optical Communications Group, Institute of Telecommunications and Multimedia (ITEAM), Universidad Politécnica de Valencia, Edifcio 8G, Ciudad Politécnica de la Innovación, Camino de Vera s/n, 46022 Valencia, Spain

M. Andrés is with Instituto de Ciencia de los Materiales, ICMUV, Universidad de Valencia, Dr. Moliner, 50, 46100 Burjassot, Valencia, Spain

E-mail: jcapmany@iteam.upv.es

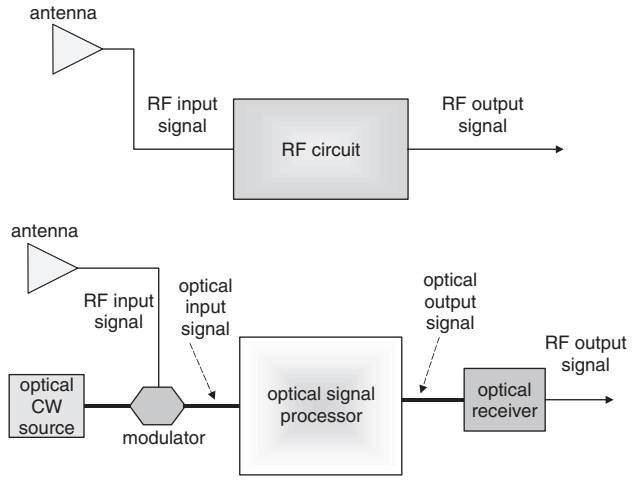

Fig. 1 *Conventional (upper) and photonic based (lower) approach to the processing of radiofrequency and microwave signals in RF systems*

6. Brings the possibility of spatial and wavelength parallelism using WDM techniques.

The potential applications for this approach (some of which will be discussed later in the paper) lay in the field of RF based services [7–11] such as: (*a*) radio over fibre (ROF) systems, mobile telephony (UMTS and 4G), wireless LAN technologies, millimetre-wave services; here the filters can be used for channel selection, channel rejection, SNR enhancement and mitigation of several effects such as fibre dispersion. (*b*) RADAR: especially in moving target identification (MTI) applications which require high performance notch filters. (*c*) Satellite communications: since being lightweight is of prime concern and notch filters are required for the suppression of cochannel interference. (*d*) Optical beamforming of phased arrayed antennas. (*e*) THz signal processing; since free space optics can provide very small delays, filters can be designed with resonances centred at the THz region of the electromagnetic spectrum.

In optical transmission systems and networks, the main application is in WDM label swapping networks [12]. Here optical channels (i.e. wavelengths) carry simultaneously baseband and RF channels by means of subcarrier multiplexing or various RF channels together by means of subcarrier division multiplexing (SCM). In this context high performance in-line optical filters can be employed to extract and filter, directly in the optical domain the content

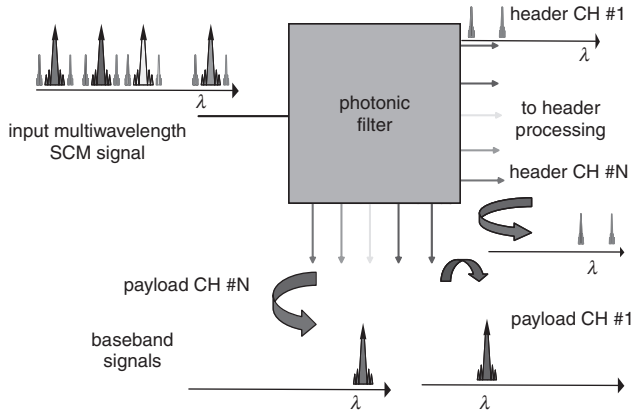

Fig. 2 *Application of photonic based microwave signal processing to optical transmission systems and networks using SCM-WDM label swapping*

of one or various RF channels within a given wavelength without distorting and affecting the baseband signal and/or other RF channels. This is shown, for instance in Fig. 2. They can also be employed to suppress part of the RF spectrum carried by an optical channels producing single sideband SSB modulation [13].

The potential applications here are: (*a*) payload and header separation in label swapping optical networks, (*b*) pilot tone extraction within WDM channels for control, protection and management purposes and (*c*) service separation in WDM transmission carrying multiple RF services within an optical wavelength. Owing to the space constraints to which the paper is subject, our main emphasis will be made on filters for RF systems and applications.

2 Review of fundamental concepts, limitations, architectures and applications

2.1 Fundamental concepts

Any filter implemented using DOPMS tries to provide a system function for the RF signal given by [63]

$$H(z^{-1}) = \frac{\sum_{r=0}^{N} c_r z^{-r}}{1 - \sum_{k=1}^{M} b_k z^{-k}} \quad (1)$$

where z^{-1} represents the basic delay between samples and c_r, b_k the filter coefficients which are implemented by optical components. The numerator represents the finite impulse part (i.e. nonrecursive or FIR) of the system function, whereas the denominator accounts for the infinite impulse part (i.e. recursive or IIR) of the system function. N and M stand for the order of the FIR and IIR parts respectively. If $b_k = 0$ for all k, filter is non-recursive and is also known as transversal filter. Otherwise the filter is recursive and it is common to use the term recirculating delay line. Fig. 3*a* shows how (1) is implemented for an N-tap transversal incoherent filter using a single optical source, while Fig. 3*b* shows the implementation using multiple optical wavelengths and a dispersive medium. To describe the filter operation we refer, for instance to the first case (Fig. 3*a*) (the discussion related to the filter structure shown in Fig. 3*b* is similar), the optical carrier $e^{j(w_0 t + \phi(t))}$, where w_0 is the carrier frequency and $\phi(t)$ is the phase noise, is amplitude modulated by an RF signal $s_{RF}(t)$. The optical modulated signal is then tapped, where each tap is differently delayed by integer values of a basic delay T and weighted by a different power coefficient a_k. After combining the samples, the receiver gets the sum of differently delayed samples to give the system response. The optical signal in front of the receiver is

$$E_0(t) = \sum_{r=0}^{N} [a_r s_{RF}(t - rT)]^{1/2} e^{j(w_0(t-rT)+\phi(t-rT))} \quad (2)$$

Equation (2) which we have deduced for a simple example of an N-tap transversal filter can be generalised to any kind of filter in the following way: For finite impulse response filters if N is a fixed integer number, while for infinite inpulse response filters (IIR) $N = \infty$. In general, the value of the impulse response coefficients is tightly related to the particular filter architecture and the optical elements used to implement the photonic tapping and time delaying.

Since (2) represents a general relationship, the detected photocurrent at the output of the microwave photonic

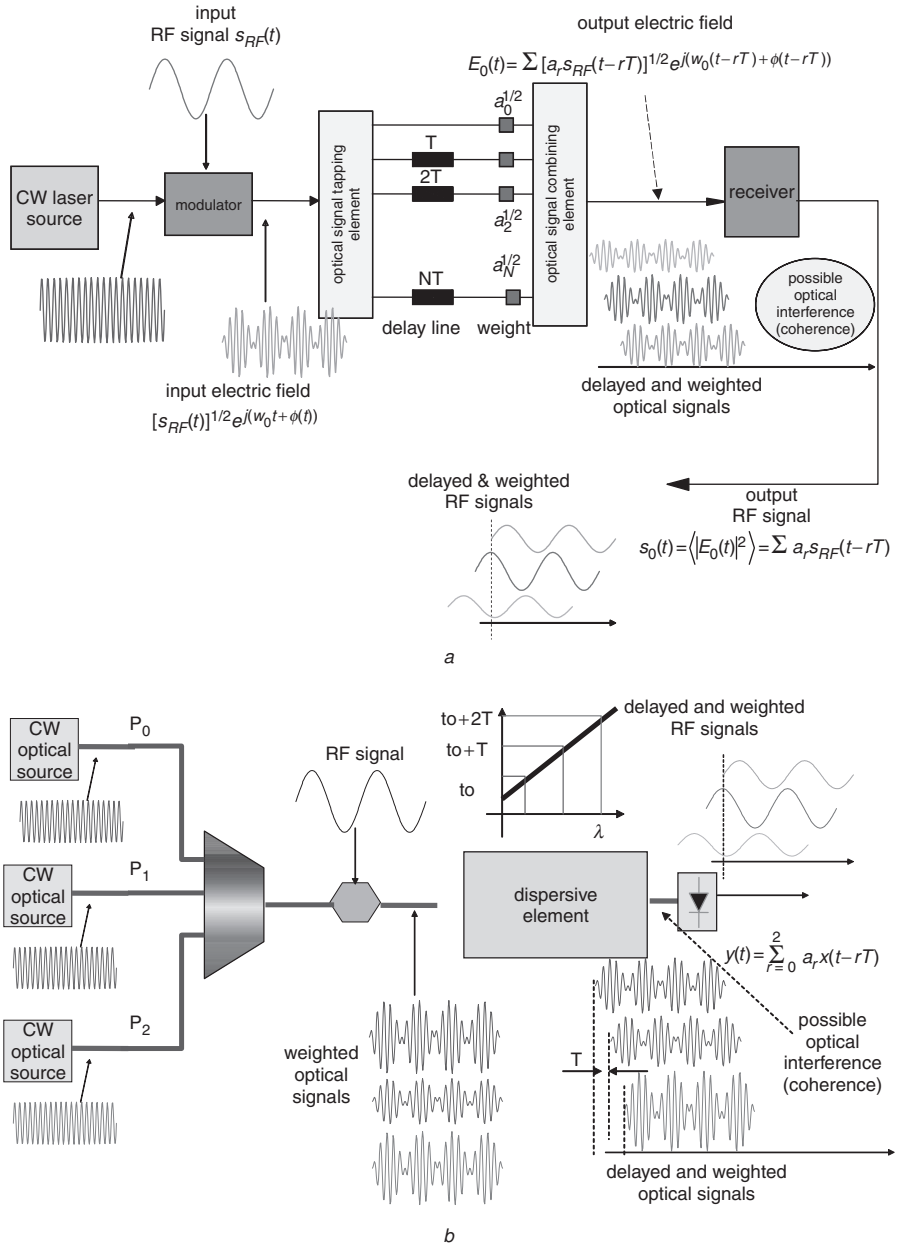

Fig. 3 *Operation of a microwave photonic filter*
a Based on fibre coil delay lines
b Based on dispersive optical elements

filter is given by

$$\begin{aligned} I_0(t) &= \Re\langle|E_0(t)|^2\rangle \\ &= \Re\sum_{r=0}^{N}\sum_{s=0}^{N}[a_r s_{RF}(t-rT)]^{1/2}[a_s s_{RF}(t-sT)]^{1/2} \\ &\quad\times\langle e^{j[-w_0 rT+\phi(t-rT)+w_0 sT-\phi(t-sT)]}\rangle \\ &= \Re\sum_{r=0}^{N}[a_r s_{RF}(t-rT)] + \Re\sum_{r=0}^{N}\sum_{s\neq r}[a_r s_{RF}(t-rT)]^{1/2} \\ &\quad\times[a_s s_{RF}(t-sT)]^{1/2}\Gamma((r-s)T) \end{aligned} \tag{3}$$

In (3), $\Re$ is the detector responsivity and

$$\Gamma((r-s)T) \propto e^{-[|(r-s)T|/\tau_{coh}]} = e^{-\pi\Delta\nu|(r-s)T|} \tag{4}$$

is the complex degree of coherence (i.e. autocorrelation) of the optical source electric field, which is related to its linewidth $\Delta\nu$ (i.e the inverse of its coherence time τ_{coh}). The first part of the right member in (3) represents the incoherent response, while the second term represents the interference arising from coherent operation.

The above expression is considerably simplified if the source linewidth is wide enough so $\Gamma((r-s)T)=0$ if $r\neq s$. This is verified if $\tau_{coh}\ll T$, that is if the source coherence time is much smaller than the basic delay provided by the filter. In such a case the filter is operating upon incoherent conditions and (3) results in

$$I_0(t) = \Re\langle|E_0(t)|^2\rangle = \Re\sum_{r=0}^{N}[a_r s_{RF}(t-rT)] \tag{5}$$

The end to end (electrical) impulse response corresponding to this situation can be directly derived from (5) yielding

$$h(t) = \sum_{r=0}^{N} a_r\delta(t-rT) \tag{6}$$

If the conditions for incoherence are not satisfied, then the filter operates in partially coherent conditions and interference arises which destroys the linear relationship between the input and output electrical signals [64]. In other words, the input and output RF signals to/from the filter cannot be related through an end-to-end electrical transfer function. Furthermore, this interference depends on the values of the optical phases of the different signal samples, which change in time due to variations in environmental conditions. For this reason, although coherent filters have been implemented in the laboratory, their practical use is difficult to achieve in practice.

Why this happens can be understood if we consider (3). Mechanical and temperature drifts in the optical structures result in changes in the optical phases experienced by the signal propagation through the filter delay lines and signal tapping elements. Since the values of the coeffients a_k in (3) are complex and directly related to these phase changes, it follows that the interference part of (3) will be highly dependent on environmental conditions and will fluctuate in time if the filter is not subject to stabilisation. For this reason there has not been as much interest in this regime of operation as compared to the work reported on filters under incoherent operation which constitute the overwhelming majority in the reported literature on microwave photonic filters. As a consequence, not much progress has been made in this area and hence, coherent microwave photonic filters will not be further considered in this paper. It must be clarified however, that considerable work has been carried in coherent photonic filters for lightwave signal processing [63], such as optical channel multiplexing and demultiplexing EDFA gain equalisation, dispersion compensation, etc. These filters should not be confused with coherent microwave photonic filters.

According to (6) the standard electrical/optical impulse response of the optical processor is represented by an equally time spaced (T) pulse train where pulses implement the filter taps. If all the samples have the same amplitude the filter is called uniform, if the samples have different amplitudes the filter is termed as apodised or windowed [63]. The electrical frequency response $H(\Omega)$ of such a structure can be obtained by Fourier transformation of the impulse response (6)

$$H(\Omega) = \sum_{r=0}^{N} a_r e^{-jr\Omega T} \tag{7}$$

The above expression identifies a transfer function with a periodic spectral characteristic as shown in Fig. 4. Note that all the filter coefficients are positive since the a_r have been defined as power coefficients. The z transform of (7), yields the desired system function given by (1). The frequency

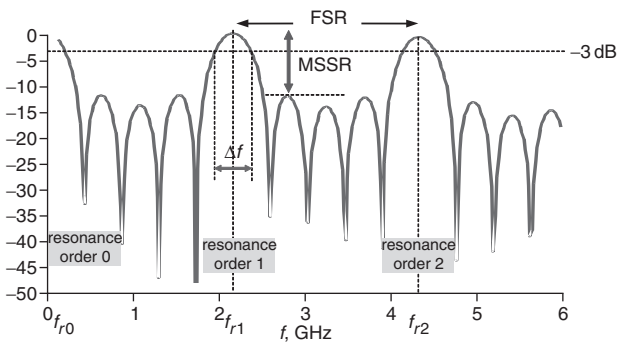

Fig. 4 *Periodic transfer functions and main parameters of a microwave photonic filter*

period is known as the filter free spectral range (FSR) which is inversely proportional to the time spacing T between adjacent samples in the impulse response. The resonance full width half maximum is denoted as $\Delta\Omega_{FWHM}$. The filter selectivity is given by its quality or Q factor which is given by

$$Q = \frac{\text{FSR}}{\Delta\Omega_{FWHM}} \tag{8}$$

The value of the Q factor is related to the number of samples (taps) used to implement it. If the number of taps is high (>10), Q factor can be approximated for uniform filters by the number of taps $Q \cong N$. This relation can be slightly corrected ($Q < N$) for apodised filters [63]. The implementation of these filters requires specific optical components to provide: (*a*) signal tapping, (*b*) optical delay lines, (*c*) optical weights and (*d*) optical signal combination, as detailed in Table 1.

Some further definitions are now introduced to complete our general description of these filters.

Filter tuneability: This property makes reference to the possibility to tune the RF bandpass position (see Fig. 4) in a sufficiently fast way. Tuneability can be achieved either in a step by step or in a continuous way, and is a key feature required to high performance flexible filters. To tune the RF response of the filter (see Fig. 4), the FSR has to be modified and therefore also the basic time delay T between samples or taps. Also the degree of frequency change or tuning produced by a given increase or decrease of the basic time delay depends clearly of the resonance or pass-band selected to be used of the structure. If we centre our discussion in fibre devices the number of techniques to produce a true time delay are quite reduced and they can be classified as:

(*a*) Switched propagation paths (switched delay lines) [65, 66]: In this technique, different paths providing different basic propagation delays (that is different values of T) can be chosen by means of an optical space switch. It allows only step by step tuneability, with the tuning speed being limited by the switching time (1–10 ms).

(*b*) Wavelength tuning of one or multiple sources combined with dispersive optical devices [26–31], [42, 58]: This technique takes advantage of currently available modern tuneable sources. The dispersive devices can be: standard fibre, high dispersive (dispersion compensating) fibre [26], linearly chirped fibre Bragg gratings (LCFBG) [27, 42, 58]. It can provide continuous or step tuneability at high speed, limited by the tuning speed of the sources (depending on the tuneable source technology from 100 ns to >100 ms).

Table 1: Components needed in a DOPMS

Function	Components
Signal tapping	2 × 2 and 1 × N, N × 1 star couplers
Optical signal combination	2 × 2 and 1 × N, N × 1 star couplers
Optical weights	Variable 2 × 2 couplers, optical amplifiers (both EDFAs and SOAs), electro-optic and electroabsorption modulators
Optical delay lines	Standard, high dispersion single-mode fibre coils and fibre Bragg gratings

(*c*) Fixed wavelength multiple sources or sliced broad-band sources combined with tuneable dispersive devices [34, 35]: This approach is based in the utilisation of novel devices with tuneable dispersion properties as special chirped FBGs with actuators to change their dispersion properties. It can provide continuous and step tuneability but in this case the time and accuracy to perform a dispersion change on the fibre device is not so well controlled (100 ms–1 s).

Filter reconfiguration: This property makes reference to the possibility of changing dynamically the values of the filter taps (c_k, b_r coefficients of (1) or a_r coefficients of (7)) to reshape its spectral response: The windowing/weighting or apodisation of the amplitude of the filter taps is also a fundamental aspect to ensure enough rejection of the avoided bands. The uniform tap apodisation (equal amplitude of the taps) provides a rejection ratio or main to secondary sidelobe ratio (MSSR) (see Fig. 4) that increases linearly with the number of taps. This can be insufficient for certain applications. Different apodisation functions have been demonstrated for MSLR improvement, either by adjusting the power of the optical sources [58], using partially reflecting FBG devices [39, 47, 55] or by controlling the attenuation/gain suffered by the taps when they travel though the optical processor [58, 67].

2.2 Limitations

Incoherent photonic filters for microwave signals must overcome a series of potential limitations prior to their practical realisation as pointed out in previous papers. The main limitations arise from:

Source coherence: The source/s spectral characteristics must be carefully chosen attending to the desired working regime. While it is true that coherent operation provides the possibility of implementing any kind of desired transfer function, these structures are very sensitive to environmental conditions as pointed above. Thus in the majority of cases, incoherent operation is employed since the filters are very compact and robust. Nevertheless, coherent effects can appear even under incoherent operation. These undesirable coherent effects may be overcome, for instance by the use of birefringent fibre delay lines [2, 6, 64].

Polarisation: Polarisation effects are mainly important under coherent operation [4]. However, it has been outlined and experimentally demonstrated that even under incoherent operation the filter can be sensitive to signal polarisation [65]. The main cause for this apparent contradiction is that some signal samples experience exactly the same delay within the filter leading to coherent interference between them even if a broadband source is employed [68]. Also, when using laser sources and external modulators, care must be taken to adjust the source polarisation to that required by the modulator. The use of polarisation preserving fibre pigtails at the modulator input helps to overcome this limitation.

Positive coefficients: In the previous Subsection it was shown that filters working under incoherent regime are linear in optical intensity but the coefficients of their impulse responses are always positive. This has two important implications as derived from the theory of positive systems [2]. The first one and more important is that the range of transfer functions that can be implemented is quite limited. The second one is that regardless of its spectral period, the transfer function has always a resonance place at baseband. This is not a serious limitation since a DC blocking filter can be inserted at the optical receiver output. Nevertheless, incoherent filters with negative coefficients can be implemented by means of differential detection [2, 21] and cross gain modulation in a SOA [69] and other recently developed techniques which will be presented later in the paper.

Limited spectral period or FSR: As it has been seen before, incoherent photonic filters for microwave signal processing are periodic in spectrum since they sample the input signal at a time rate given by T. Thus the spectral period or FSR is given by $1/T$. If the filter is fed by only one optical source then, as it was shown in Section 2.1, the source coherence time (which is inversely related to the source linewidth) limits the maximum (minimum) value of the attainable FSR under incoherent (coherent) operation. To overcome this limitation it has been proposed to feed the filter with arrays of independent optical sources [57–59].

Noise: As far as the optical source is concerned, passive filters behave as frequency discriminators and thus convert the optical source phase noise into intensity noise which materialises into RF baseband noise at the filter output [70–75]. This conversion is dependent on the operation regime. For incoherent operation the noise is periodic in spectrum showing notches at zero frequency and multiples of the filter FSR. Under active operation (i.e. when incorporating optical amplifiers) new RF noise sources appear as a direct consequence of the beating between the signal and the spontaneous emission [74, 75]. It has been proved however that the converted phase noise is still the dominant noise source [75]. The use of source arrays to feed the filter is an attractive solution to overcome noise limitations [58]. This is due to the fact that signals recombining at the photodetector at different wavelengths will generate the intensity noise centred at the frequency resulting from the beats of the optical carriers. Since these have very high values they will be filtered out by the receiver.

Reconfigurability: As defined previously, this property refers to the possibility to dynamically change the values of c_r and b_k in (1). Passive structures are incapable of this feature. Several solutions have been proposed to overcome this limitation including the use of optical amplifiers [17–19], modulators fibre gratings and laser arrays [54–62].

Tuneability: As defined previously, this property refers to the possibility to dynamically change the position of filter resonances or notches. To provide tuneability it is necessary to alter the value of the sampling period T. Solutions that include the use of switched fibre delay lines, fibre Bragg gratings or other tuneable tap schemes have been proposed, as will be presented below.

2.3 Architectures

Figures 5*a*–*d* illustrates four possible different approaches for the implementation of incoherent microwave photonic filters attending to the type of source/sources employed, the minimum time delay difference between taps and the maximum attainable FSR. Figure 5*a* shows the first possibility, where only one modulated optical source is employed. The filter taps are therefore implemented from delayed versions of the output signal from this source. Using high quality (low linewidth) sources results, as it has been explained before, in the limitation of

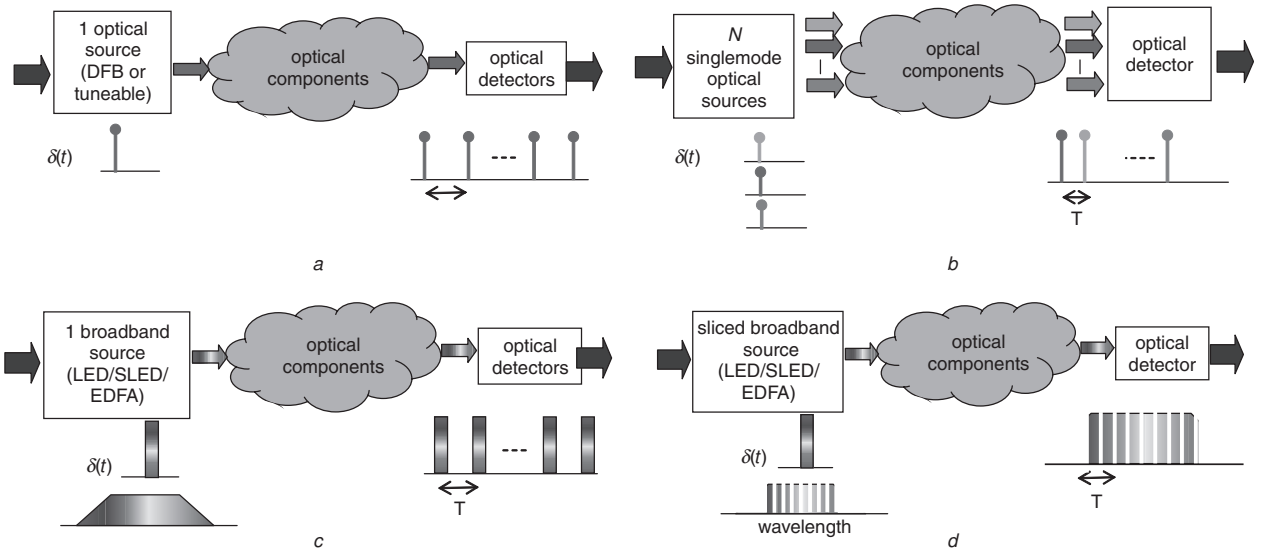

Fig. 5 *Different architectural possibilities for the implementation of microwave photonic filters*

a One optical source
b *N* singlemode optical source
c One broadband source
d Sliced broadband source

the maximum achievable value for the filter FSR if interference effects need to be avoided. The alternative to increase the filter FSR is to use single-mode sources with moderate linewidth such as low quality DFB lasers. This is illustrated in Fig. 5*b*, where multiple (N) optical sources (lasers) modulated by the same RF signal are used to implement the filter. Each source implements only one or a limited set of taps. If the sources implement only one sample of the filter impulse response no phase correlation between samples, so this approach is equivalent to that of Fig. 5*a* using a zero coherence time source and, therefore, there will be no limitation in the minimum time delay or maximum FSR. In the second case, that is if each source in the array implements a limited set of samples, interference between delayed versions of the samples produced by the same source may arise, but it can be avoided if adjacent samples of the impulse response are generated different sources and the time separation between two consecutive samples generated by the same source (i.e. NT) is much bigger than the source coherence time.

A third alternative is shown in Fig. 5*c*. Here a modulated broadband optical source (LED, EDFA or SOA ASE source, etc) with very low coherence time (almost zero) is employed to generate all the filter taps. Therefore, each tap carries all the spectral components of the broadband source. Hence since the source linewidth can be considered almost infinite, the coherence length of each tap is zero and there is no limitation in the minimum time delay or maximum FSR. An important limitation appears if the filter delays are provided by dispersive elements. Since each sample is carried by a broadband source, the exact value of the delay is affected, not only by first-order dispersion, but also by second-order dispersion of the delay line. This can lead (as will be shown later in the paper) to an undesired low-pass envelope effect affecting the overall filter transfer function.

A final option is shown in Fig. 5*d* which is similar to the previous case, the only difference is that the broadband optical source is sliced. Here each tap is implemented by a different part of the sliced spectrum. If each slice is carried by a portion of optical spectrum broad enough then, as in the previous case, there are no limitations in the filter FSR.

To date two main approaches have been followed by most of the research groups throughout the world to implement the delays lines of incoherent microwave photonic filters, these are:

(*a*) Using fibre coils as delay lines together with single/multiple sources and signal tapping combination and weighting by means of discrete fibre or integrated optics components. We will refer to these as FDLFs (fibre delay line filters)
(*b*) Using fibre gratings as delay lines and/or weighting elements in conjunction with single or multiple tuneable source arrays. We will refer to these as FGDLFs (fibre grating delay line filters).

2.4 Applications

Microwave photonic filters are of interest in a wide variety of applications. Figure 6 shows a diagram where some of the most interesting are depicted. For instance, in radio over fibre systems, these filters can find applications both for

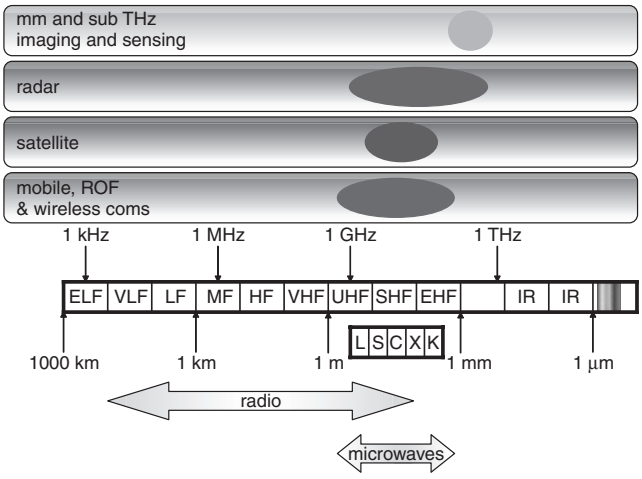

Fig. 6 *Diagram showing some of the most interesting applications of microwave photonic filters in the RF spectrum*

channel rejection as well as for channel selection [7–11, 75]. In the first case (channel rejection), we deal with an optical link where not only the desired signal is carried by the fibre, but also unwanted interfering signals that are also picked up by the antenna. For example, in radio astronomy applications [75] the signal transmission from several stations to a central site requires the removing strong man-made interfering signals from the astronomy bands. The ability to reject these interfering RF signals directly in the optical domain is an unique characteristic of these photonic filters [7]. Another application example is for noise suppression and channel interference mitigation in the front-end stage after the receiving antenna of an UMTS base station prior to a highly selective SAW filter [8]. In the second case (channel selection), the signal carried by the optical link is composed of a frequency plan that comprises several disjoint parts of the RF spectrum (UMTS, HIPERLAN, LMDS). Here, a bandpass photonic filter can be employed to select a given RF band or spectral region [9]. Furthermore, the selected band can be changed if the filter is tunable. In both cases the position of the frequency notch or the filter bandpass can be as low as a few MHz or as high as several tens of GHz due to the broadband characteristics of photonic delay lines. Photonic filters for RF signals can also be of interest for applications where lightweight is a prime concern, for example analog notch filters are also needed to achieve cochannel interference suppression in digital satellite communications systems [10].

Another range of applications benefit from this approach as it solves current bottlenecks in the electronics. For instance in moving target identification (MTI) radar systems [1], the Doppler effect is used to separate targets of interest from clutter. The filtering of clutter and noise (the unwanted signals) is performed using a digital notch filter placed after frequency downconversion to baseband and analog to digital (ADC) conversion. Figure 7 illustrates a typical example. To distinguish the small echo from the target from large echo from the fixed objects high performance (14–18 bit resolution) ADCs are required which represents a major bottleneck in the system. If the clutter can be removed directly in the optical domain by means of a photonic filter, then the high resolution requirements on the ADCs can be relaxed. For example, with a 30 dB clutter attenuation the required ADC resolution is reduced by 5*b*.

The use of broadband photonic delay lines to the feeding of phased-array antennas is also an extremely advantageous application. The configurations employed for the optical feeding of true time delay phased arrayed antennas are identical to those employed in the implementation of incoherent transversal microwave photonic filters (see Figs. 3 and 4), the only difference being that signal taps are detected by different photoreceivers.

3 Recent advances in high performance incoherent filters

3.1 *Transversal filters based on the optical tap wavelength tuneability*

High performance and programmable RF transversal filters can be obtained employing both LCFBGs or fibre coils as dispersive media in combination with an array of optical sources [56–59]. The layout of the filter for a specific case of a laser array of five elements is shown in Fig. 8, although in general it is composed of N sources. The advantage of using a laser array to feed the delay line is

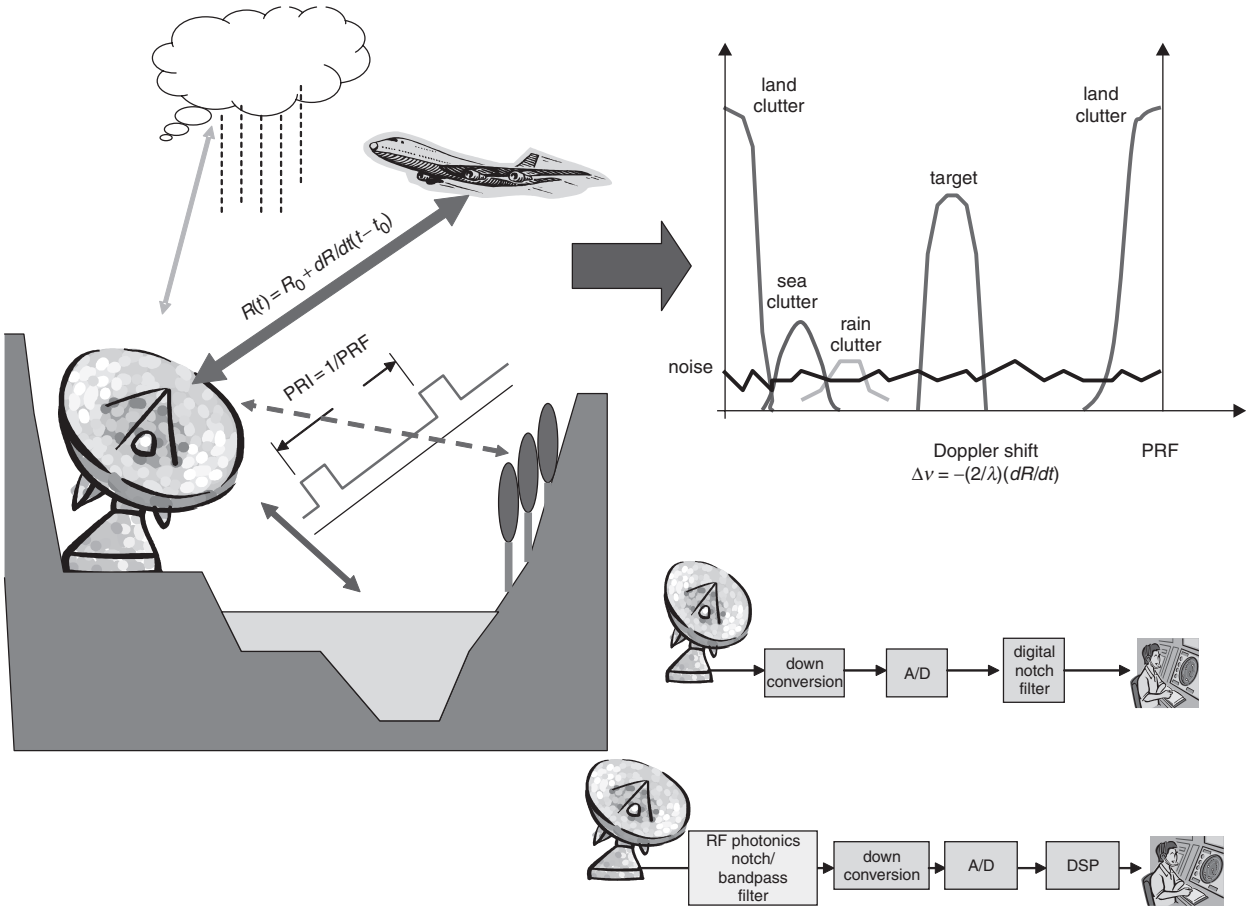

Fig. 7 *Illustration of the use of microwave photonic filter for noise and clutter elimination in MTI radar systems*

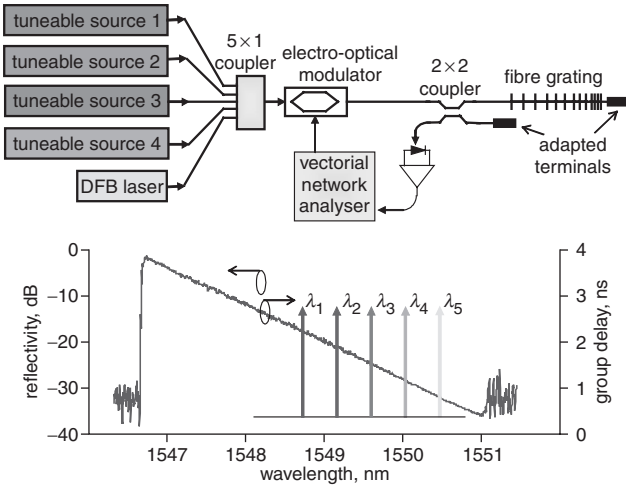

Fig. 8 *Architecture of a tuneable and reconfigurable RF photonic filter*

Using a laser array and a LCFBG

twofold. On one hand, the wavelengths of the lasers can be independently adjusted. Thus signals carried by wavelengths with an equal spectral separation representing the RF signal samples can be fed to the fibre grating suffering different delays, but keeping constant the incremental delay T between two adjacent wavelengths emitted by the array if the delay line is implemented by means of a linearly chirped fibre grating. This means for instance, and referring to Fig. 3*b* that the delay between the signals at λ_1 and λ_2, λ_3, λ_4, λ_5, ..., λ_N is respectively T, $2T$ $3T$, $4T$ and $(N-1)T$. Hence the configuration can act as a transversal filter, where the basic delay is given by T. Furthermore, T can be changed by proper tuning of the central wavelengths emitted by the laser array. Thus, this structure provides the potential for implementing tuneable RF filters.

The second advantage stems from the fact that the output powers of the lasers can be adjusted independently at high speed. This means that the time impulse response of the filter can be apodised or in other words, temporal windowing can be easily implemented and therefore the filter transfer function can be reconfigured at high speed. We have experimentally succeeded in the demonstration of both tuneability and reconfigurability. For instance, Fig. 9 shows the results when the samples of the five-stage uniform filter were apodised by a truncated Gaussian window. The upper trace at Fig. 9*a*, shows the spectrum corresponding to the uniform filter (i.e. unapodised) where the normalised output powers from the lasers in the array is [1 1 1 1 1]. The lower trace corresponds to a five-stage Gaussian windowed filter where the normalised output powers from the lasers in the array is given by [0.46 0.81 1 0.81 0.46]. Fig. 9*b* demonstrates the resonance tuneability, increasing the resonance position from ~ 2 up to 4 GHz (i.e. reducing in a factor of two the wavelength separation). In addition, this Figure shows the carrier suppression effect (CSE) suffered by the second resonance in this specific case of dispersive media and wavelength spacing. CSE is a well known limiting effect in analog fibre optic transmission due to the fibre chromatic dispersion which results in the fading of several RF frequencies at the output of a dispersive fibre link. This fading is due to the destructive interference between the modulating RF sidebands upon mixing with the optical carrier at the photodetector. The destructive interference is obtained for those RF frequencies for which fibre dispersion results in a π phase shift between the two sidebands after propagation. This effect can be overcome using single sideband modulation at the filter input.

An additional advantage of employing laser arrays is the possibility of exploiting WDM techniques for parallel signal processing [60]. The possibility of implementing a bank of parallel transversal filters is feasible by extending the concept of a single fibre-optic RF transversal filter based on multiple LCFBGs and dispersive elements into the implementation of a bank of transversal filters, by means of utilising wavelength division multiplexing techniques. This technique allows for the simultaneous processing of a single RF signal by various filters.

Laser arrays are at present time a costly solution although there have been attempts for their integration in a single chip and future work driven by WDM applications will most probably reduce their cost. In the meantime however, the use of more economical optical sources has been investigated in order to provide lower cost solutions. For instance, a high performance and continuously tuneable RF-filter with larger FSR tuning range and simple tuning scheme was

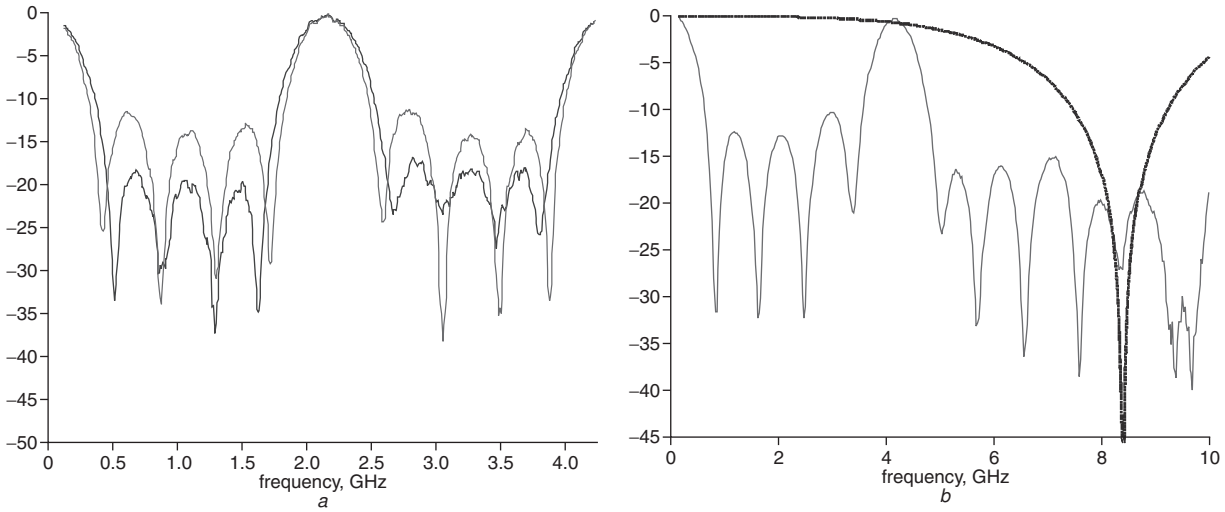

Fig. 9 *Results of the architecture using a laser array and a LCFBG*

a The upper trace: Uniform filter (i.e. unapodised) output powers from the lasers in the array is [1 1 1 1 1]. The intermediate trace: 5 stage Gaussian windowed filter where the normalised output powers [0.46 0.81 1 0.81 0.46]

b Resonance tuneability, resonance position from ~ 2 up to 4 GHz and detail of the carrier suppression effect (CSE). Both curves show $|H(f)|^2$ as a function of the frequency

presented in [35]. This filter consists of a broadband optical source, i.e. a super-electroluminescent diode, SLED, and uniform fibre Bragg gratings as filtering elements. This approach was previously demonstrated to provide a simple tuneable notch filter where the broadband optical source was sliced by means of only two FBGs, which can be tuned by means of a strain application stage [34]. The output light of the source is driven to the FBG through an optical circulator, and therefore, the reflected signal will be driven to the rest of the system. The uniform FBGs are 5 cm long written in a series configuration, as shown in Fig. 10, and they will be stretched to tune the reflection bandwidth, initially centred at λ_{init}. Since the central optical frequency, ω_N, of different gratings must be equidistant [35], each grating must be stretched over a different fibre length: $L_N = L/N$, so the total device length is determined by the number of optical taps.

The device employs identical Bragg gratings, the central wavelengths of these devices, λ_{init_N}, have been tuned and fixed by the application of a mechanical tension before gluing the gratings on the mechanical stage. One of the gratings is not glued on the stage but the others are glued over a fibre length given by: $N = 0$, not stretched, $L_1 = 21$, $L_2 = 10.5$ cm and $L_3 = 7$ cm. The inset of Fig. 10 shows the wavelength tuneability of all four optical taps corresponding to reflected signals by the gratings when different elongations are applied. The lowest wavelength is kept constant (the grating is not stretched) and the others show a linear behaviour, in such a way all of them are equidistant for different elongations.

Figure 11 shows the measured RF-transfer function of two filters corresponding to optical tap spectral spacing of 1.20 and 0.65 nm and a fibre length of 23 km as the dispersive element, together with the theoretical calculation. The filter free spectral range, FSR, were 2.19 and 4.05 GHz, respectively, although the FSR tuning range was demonstrated to be 1–6 GHz.

A similar configuration for a four-tap filter where the gratings are written in a parallel configuration to achieve large sidelobe suppression by weighting the taps was also proposed in [35]. Figure 12 shows the new configuration of the gratings, which features larger flexibility in the implementation of the filters with the only drawback of larger optical losses, which were compensated by the optical amplifier. The gratings were written in different arms of a 4 × 4 optical coupler and glued onto the mechanical stage over different fibre lengths, as explained above. As known from filter theory [58], the shape of the transfer function of a discrete time transversal filter can be changed or reconfigured by changing the optical power of the different taps according to an apodisation function. Therefore, a decrease in the secondary sidelobes of the filter can be achieved. The optical signals corresponding to the side taps (in our case, $N = 0$ and $N = 3$) went through a two-input variable attenuator, which could be varied according to the desired degree of MSLR of the RF-filter.

Figure 13 shows the measured main to sidelobe ratios of implemented RF-filters by introducing different attenuation values to the optical signal taps, together with the theoretical curve. As an example, the intensity of the four taps of two filters is shown in two different insets, exhibiting different apodisation profiles. The uniform intensity pattern leads us to the theoretical (and measured) limitation of 11.3 dB (see Fig. 11) and sidelobe reduction has been demonstrated in these filters up to 25 dB.

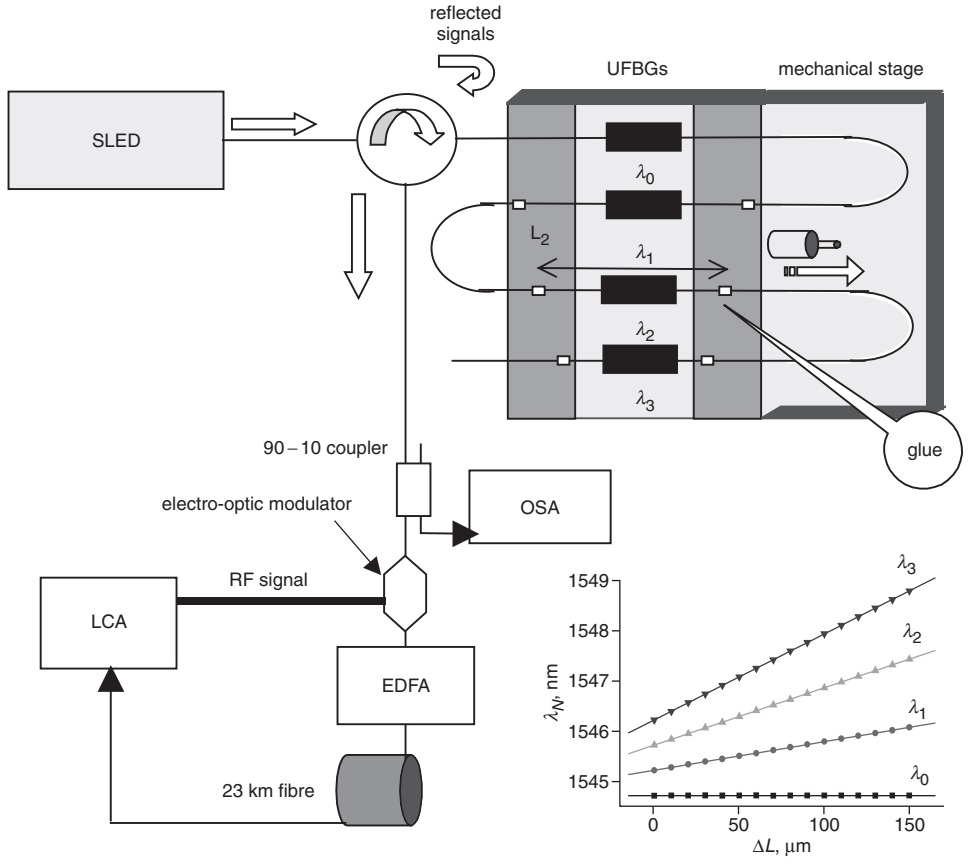

Fig. 10 *Setup of the flexible uniform FBG-based RF filter*
Inset: Spectral position of the reflectivity peaks (filter taps) when the fibre is stretched

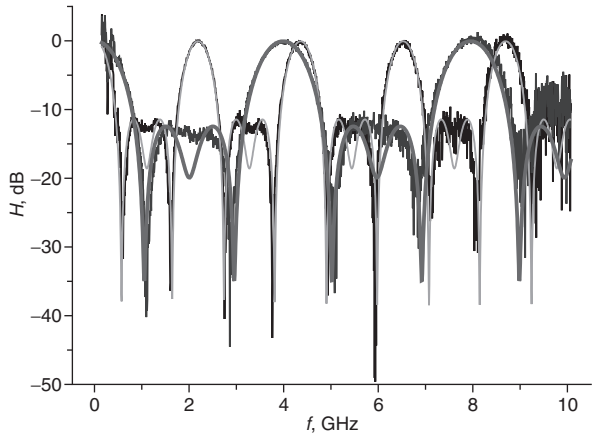

Fig. 11 *Tuneability of the RF-filters*

Experimental (black: filter 1, blue: filter 2) and calculated (green: filter 1, red: filter 2) filter response against RF signal frequency with different spectral spacing between taps

Another interesting option is to employ AWG devices with high port count in order to implement source slicing with a high number of samples [67, 76]. With this technique we have recently reported a 12-sample transversal filter using a two-stage 1×40 AWG configuration shown in Fig. 14. This structure has the advantage of also allowing filter reconfiguration if switches or variable attenuators are placed in between the demultiplexing and the multiplexing stages. (We have already demonstrated this double functionality. The work is still under peer review.)

In the structure above, the combinations of the SLED and the EDFA sources provides an almost flat optical spectrum which is spectrally sliced by the following two AWGs. The proper channel by channel interconnection between AWGs provides a certain degree of freedom to select the wavelength spacing between the slices. The employed AWGs were designed for DWDM applications with 0.8 nm spacing between adjacent channels and 0.4 nm of 3 dB optical bandwidth. Figure 15 shows two examples of channel interconnections to provide different RF lobe tuning and RF lobe 3 dB bandwidth. Proper optical attenuation of the interconnections provide the feasibility of taps apodisation to reduce the sidelobe level. The reader should notice the low pass filtering effect arising from the combined use of broadband slices (0.4 nm) and high dispersion and, on the other hand, also the effect of the dispersion slope (S) and the large wavelength range covered. This phenomenon manifests as an amplitude reduction and a RF lobe bandwidth increasing for higher RF frequencies as it can be observed from results in Figure 15, and it was extensively discussed in [67].

Other recently reported slicing technique employs a fibre Bragg grating and an acoustic wave, which generates the optical taps when it is propagated along an uniform FBG [77]. The acoustic wave creates a periodic strain perturbation that modulates periodically the period and the refractive index of the FBG. In this system, the spontaneous emission of an EDFA around 1540 nm is used as a broadband source, the FBG is written at the neck of a symmetric tapered fibre to increase the efficiency of the acoustic interaction and the longitudinal acoustic wave is generated by a piezoelectric transducer driven by an RF signal and launched into the fibre using a silica horn. It produces spectrally equispaced bands of reflection on both sides of the original Bragg grating as we can observe in Fig. 16.

By using a SMF-28 fibre length of 46 km as a dispersive element, two transversal filters were implemented with the acoustic frequencies of 0.755 and 1.444 MHz. The wavelength spacing of the optical taps were 0.11 and 0.22 nm, respectively and the RF filter characteristics are shown in Fig. 17. The former showed a FSR of 6.25 GHz and a 3 dB-bandwidth of 1.44 GHz, whereas the second one had a FSR of 11.5 GHz and a 3 dB-bandwidth of 2.76 GHz. The reconfigurability of the filter can be obtained by applying different voltages to the piezoelectric transducer since different degrees of apodisation of the optical taps intensities are achieved by controlling the acoustic power. A main to side lobe ratio up to 20 dB has been demonstrated.

However, in RF applications when an optical signal is used to carry several RF signals providing different services, and photonic filters are used to select one of these services, as happens in next generation optical access networks, there is a need for obtaining a single and very selective tuneable radiofrequency band in sliced broadband optical source [78]. The presence of a periodic transversal filter response where different RF bands are selected by the filter implies a limitation in the number of services carried by the same optical carrier. Thus, a new approach to obtain single bandpass RF filters is extremely interesting for their implementation in optical access networks. It is based on a broadband optical source and a fibre Mach-Zehnder (MZ) interferometer, as shown in Fig. 18. When the source optical output is transmitted by the interferometer and launched into a fibre delay line, a tuneable bandpass filter

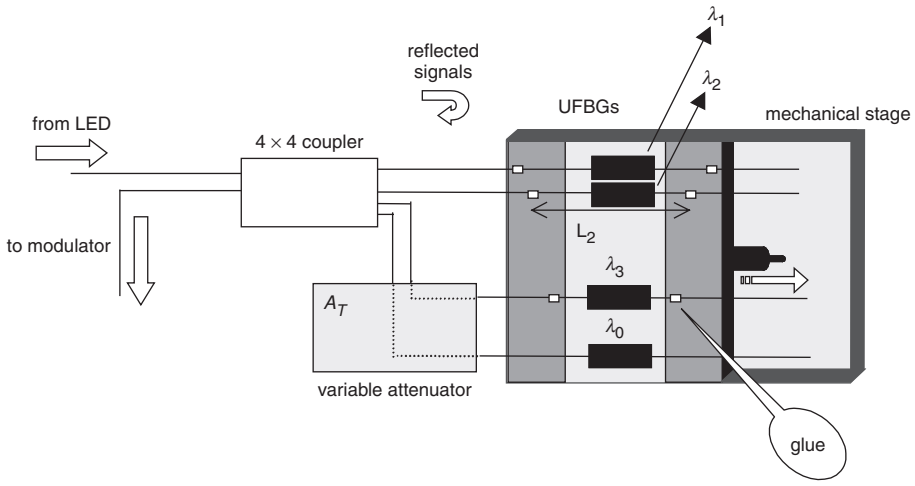

Fig. 12 *System configuration for reconfigurable sidelobe suppression*

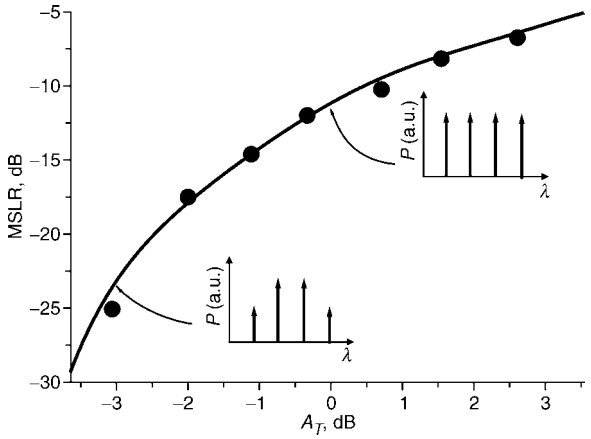

Fig. 13 *Calibration curve of sidelobe suppression against attenuation tuning parameter*

Insets: Intensity of the taps in different filter

is achieved showing a single bandpass frequency response, large tuneability without changing the bandwidth of the filter and high attainable Q values.

The experimental arrangement is given by Fig. 18. The spontaneous emission of an erbium doped fibre amplifier (EDFA) is used as a broadband optical source, with a 3 dB bandwidth of 5.4 nm and the Mach-Zehnder interferometer leads to obtain different spectral periodicities $\Delta\omega$. In this system, a 46 km fibre length is used as dispersive element, and the RF filter response shows a bandpass characteristic centred at the frequency Ω_0, that can be tuned varying the periodicity $\Delta\omega$ of the interferometer Mach-Zehnder. As shown in Fig. 19, periodical wavelength spacing in the interferometer output of 0.237 and 0.173 nm lead to bandpass filters at 5.83 and 7.88 GHz. A tuning range of several tens of GHz was achieved with a main to secondary lobe ratio (MSLR) lower than 20 dB and the Q maximum value achieved around 40. Note that the filter is no longer periodic, since the Mach-Zehnder does not operate as a discrete but as a continuous (i.e. sinusoidal) slicing filter. Thus the spectral response will only contain two resonances, one placed at baseband and another paced in the RF region centred at a frequency, the value of which depends on the Mach-Zehnder path delay imbalance.

The Q factor is plotted in Fig. 20 for several RF filters implemented with different wavelength periodicity $\Delta\lambda$ of the signal at the EOM input, for two different dispersion values according to 23 km (■) and 46 km (●) length of

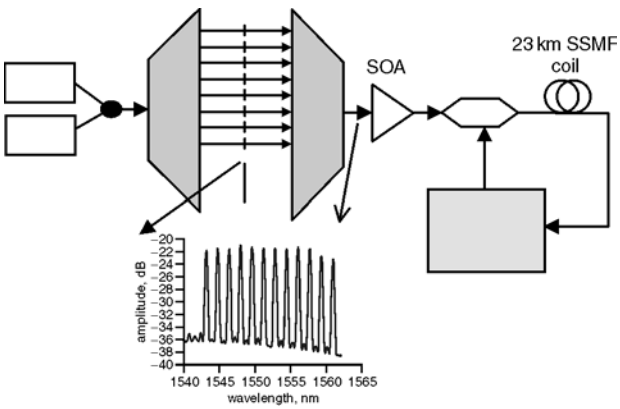

Fig. 14 *Spectral slicing technique employing AWGs*

Inset: Sliced spectrum employing 12 channels of the AWGs

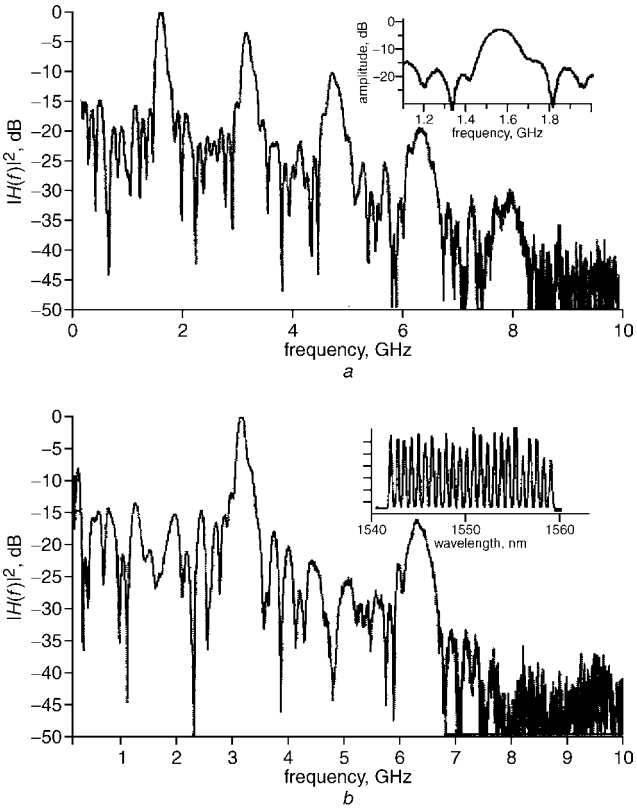

Fig. 15 *RF amplitude and response*

a Normalised RF amplitude for the sliced spectrum. Slices from 1543.7 to 1561.3 nm up to a total number of 12 bands (samples), 1.6 nm apart one to each other. The RF response presents a band spacing of 1.56 GHz. Inset: Precise measurement of the 1° pass-band

b Normalised RF response for 24 slices (1542.9–1561.3 nm), with 0.8-nm wavelength spacing. FSR = 3.1 GHz; MSLR = 14 dB; 3 dB bandwidth of 125 MHz, Q factor = 24.8

fibre. The dashed curve plots the Q factor that can be achieved by a Gaussian optical source of 5.4 nm 3 dB bandwidth. As shown, Q value is improved by increasing the optical source linewidth although the influence of the dispersion slope drives to a degradation of the radio-frequency response. Therefore, potential high Q values can be achieved by choosing a broadband source with a suitable linewidth and reducing the dispersion slope. This can be achieved by using two different fibres to compensate the dispersion slope. The dotted line shows the Q factor when the dispersion slope is compensated.

As we have pointed out in the previous Section, one of the main limitations of incoherent transversal filters is that only filters with positive taps can be implemented, since the intensity is a positive magnitude. Some solutions have been reported to overcome this limitation, from the opto-electronic approach that uses differential detection [21] to various configurations which use active elements to generate negative taps, i.e. amplitude inversion due to gain saturation in the homogenously broadened gain medium of a semiconductor optical amplifiers (SOA) [79], carrier depletion effect in a DFB laser diode [80], cross-intensity modulation of the longitudinal modes of an injection-locked Fabry-Perot laser diode [81]. For example, microwave filters based on wavelength conversion employing cross-gain modulation of amplified spontaneous emission spectrum (ASE) of a SOA have been demonstrated [82]. Recently, a new low-cost approach based on passive elements is proposed to generate negative taps is based on filtering a broadband source with the transmission of uniform fibre Bragg gratings (FBG) [83].

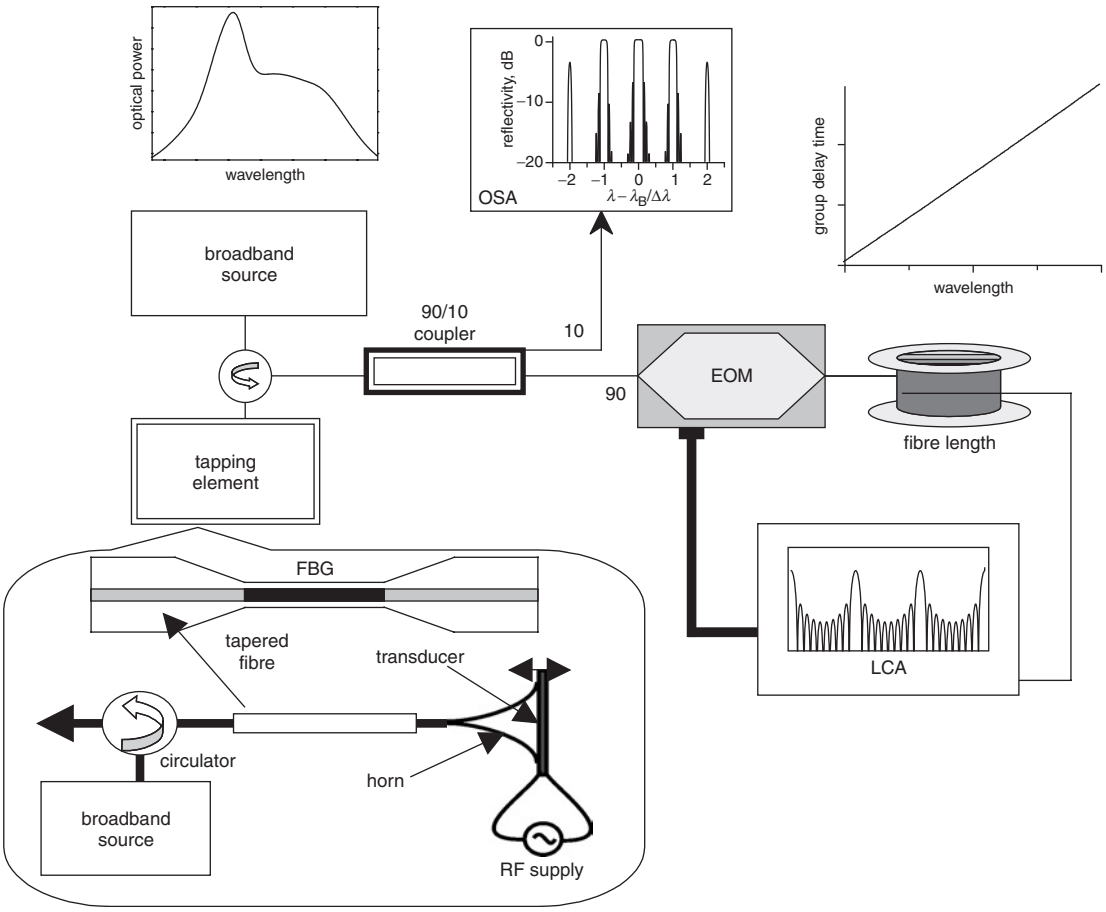

Fig. 16 *Experimental setup to implement transversal filters consisting of a Bragg grating-based acousto-optic superlattice modulator*

The implemented filter is formed by a tuneable laser (TL) and the signal transmitted by a uniform FBG, which is illuminated with the ASE of an erbium doped fibre amplifier (EDFA). The broadband optical source has a 3 dB bandwidth of 5 nm around 1530 nm. The uniform FBG is 1 cm-long with Bragg wavelength of 1530.96 nm and maximum reflectivity of 8 dB. The output light of the FBG and the TL are driven to a 90/10 optical coupler. The combined signal can be monitored by an optical spectrum analyser, OSA, by using the 10% arm. The 90% arm signal is amplitude modulated in the EOM, by a RF-signal of frequency f generated by a lightwave component analyser, LCA. A fibre length of 46 km will be the dispersive element in the filter, and finally, the transfer function of the filter is measured in the LCA (Fig. 21).

Figure 22 gives the measured and theoretically predicted free spectral range of 2-taps RF filter against different wavelength spacing between the central Bragg wavelength of the FBG and the TL output signal showing tuneability in the 0.7–5.6 GHz.

To show the good performance of these filters when various taps are added, a five-taps RF filter has been

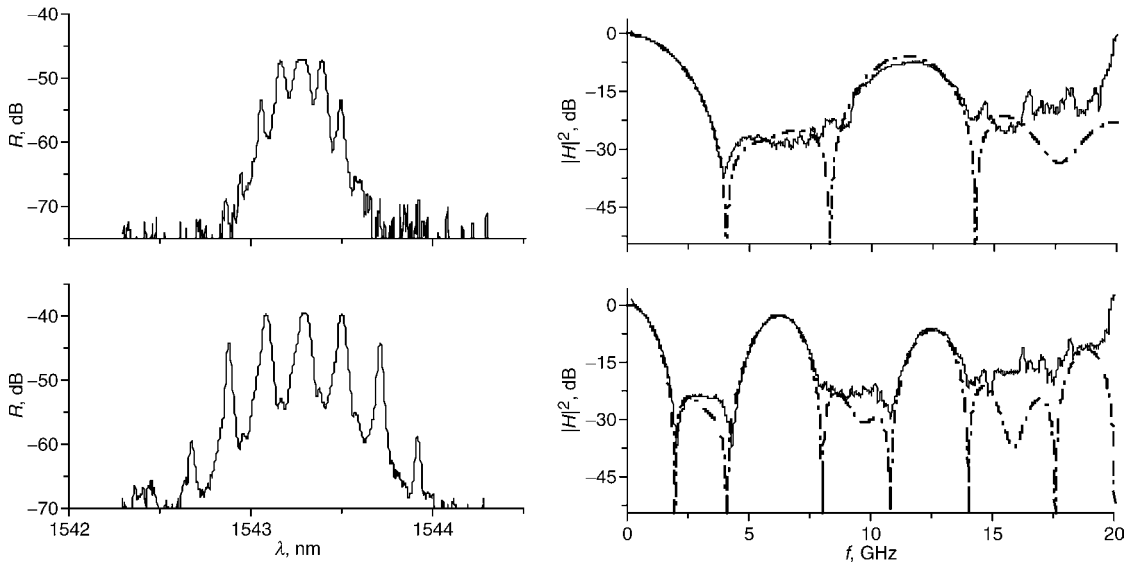

Fig. 17 *Experimental setup to implement transversal filters consisting of a Bragg grating-based acousto-optic superlattice modulator*

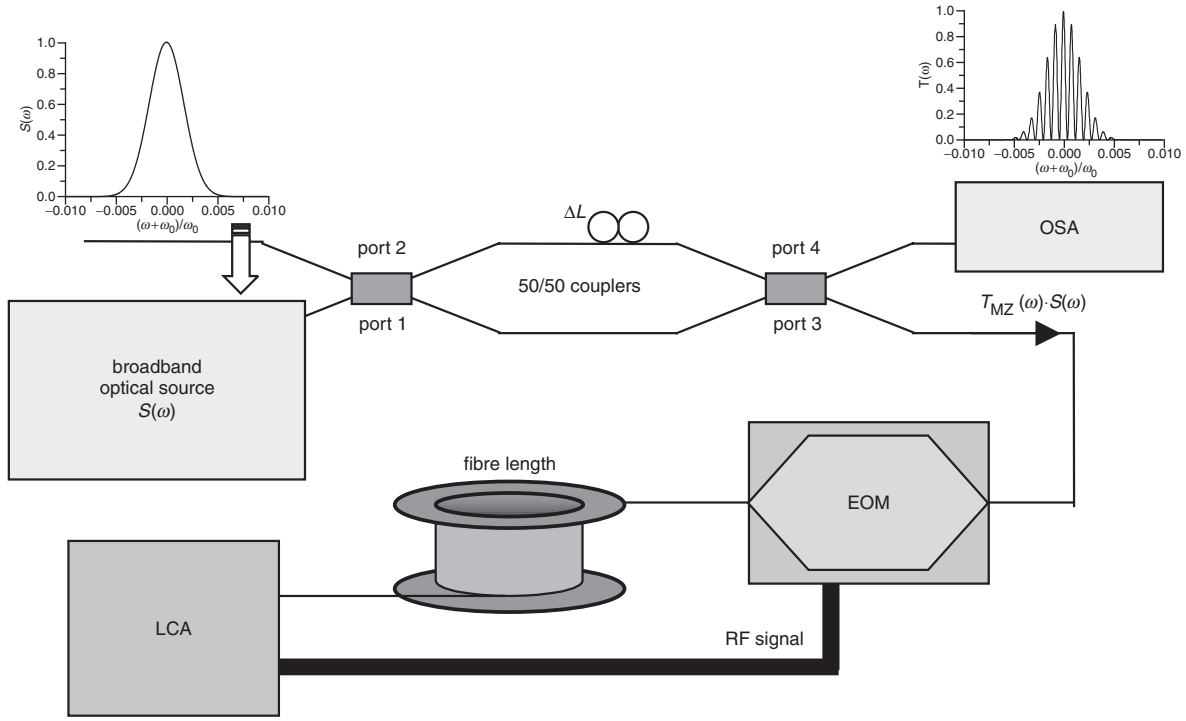

Fig. 18 *Schematic of the implementation of the RF single bandpass filter based on a broadband source and a Mach-Zehnder interferometer*

measured using two FBGs and three lasers in which wavelength separation is 1.16 nm (Fig. 23). As it can be appreciated, the system shows a broad tuning range and a good performance of the transversal filter.

We have also proposed within the framework of the IST project LABELS a different and promising technique to obtain RF filter with negative coefficients [84] which is based on the counter-phase modulation in a Mach-Zehnder external modulator devices by means of employing the linear part of the transfer function with positive and negative slopes. The concept is illustrated in the upper part of Fig. 24 with a simple RF modulating source.

The upper left part of the Figure depicts the typical output against input optical power sinusoidal transfer function of an electro-optic Mach-Zehnder modulator (EOM) as a function of the applied bias voltage VBIAS. Two linear modulation regions with opposite slopes can be observed centred at V_{BIAS}^{-} and V_{BIAS}^{+}, respectively. As shown in the right part of the Figure, the same RF modulation signal applied to the modulator at each of the former bias points will produce an optical modulated output signal with the same average power but where the modulating signals are

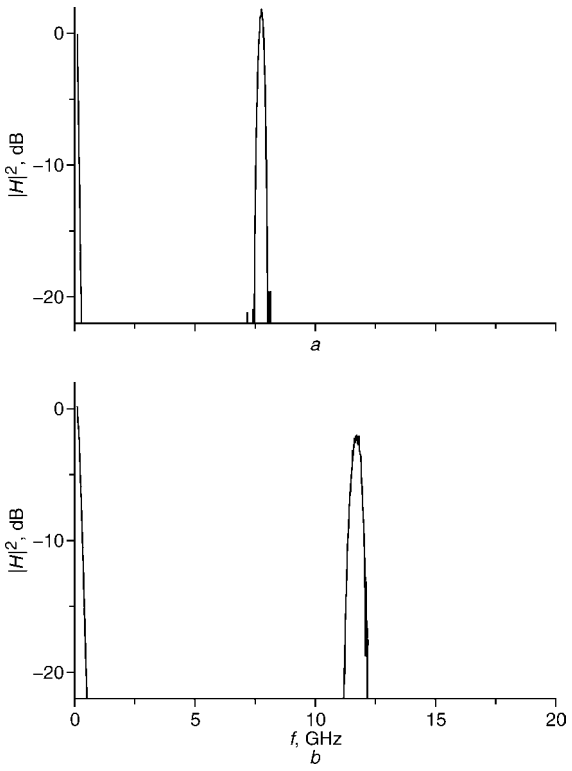

Fig. 19 *Response of the RF filters implemented by a 46 km of fibre*

a 0.237 nm
b 0.173 nm

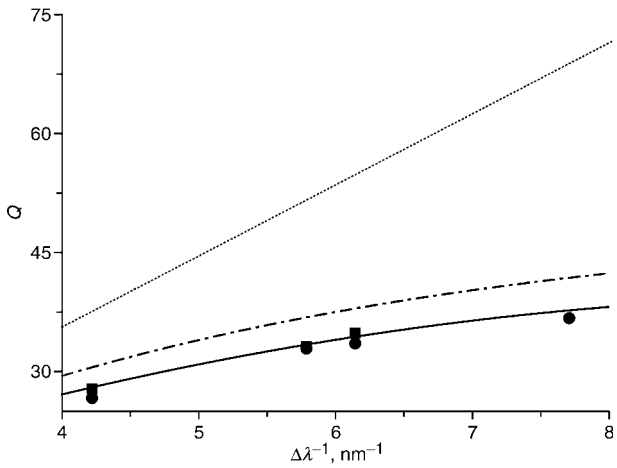

Fig. 20 *Dependence of the Q factor of a RF filter on the wavelength periodicity Δλ of the signal at the EOM input*

For two different dispersions L_1 (■) and L_2 (●). Solid line: Theoretical fit of the experimental data. Dashed line: Q factor obtained when optical source (bandwidth of 5.4 nm) is Gaussian. Dotted line: Q factor obtained when dispersion slope is compensated

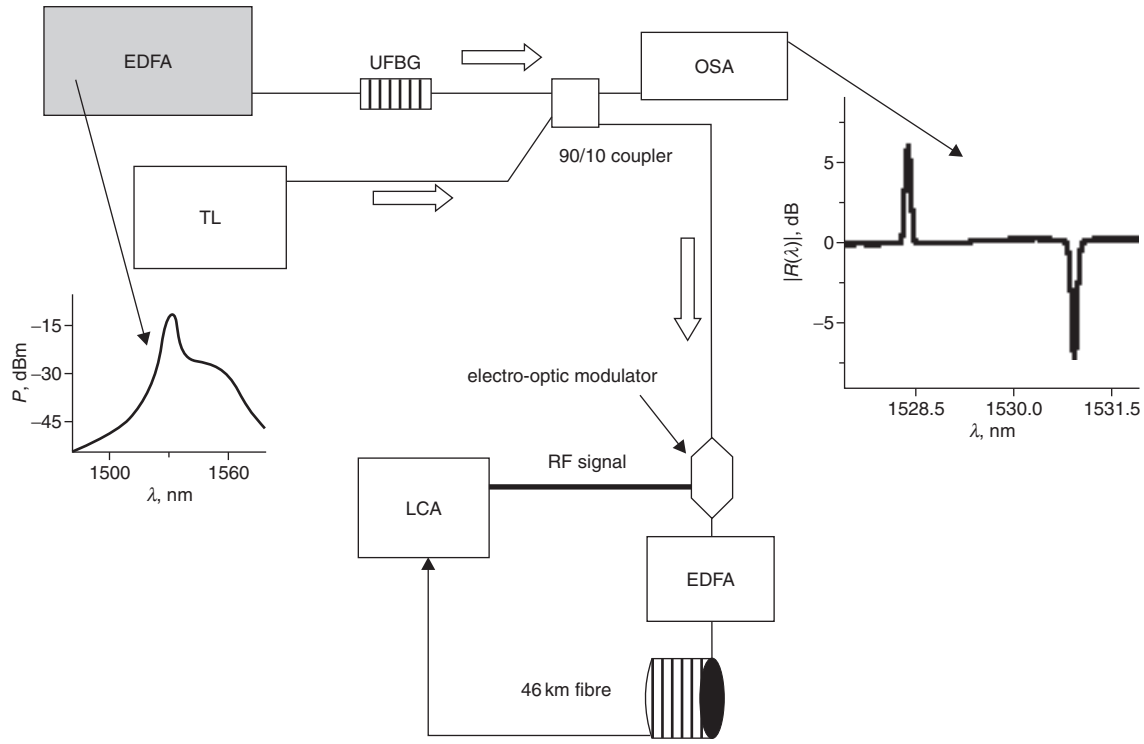

Fig. 21 *Setup of the RF negative-taps filter*
Inset: Input signal launched into EOM relative to EDFA power level

180° shifted or in counter-phase. In other words they can be considered of different signs. This principle can be employed to implement RF photonic filters with negative coefficients if the output wavelengths from a multiwavelength source (either a laser array or a sliced broadband source) are applied to a MZ modulator biased at either V^{+}_{BIAS} or V^{-}_{BIAS} depending on whether they are employed to implement positive or negative filter samples. The output from both modulators are combined and sent to a dispersive element (i.e. a LCFBG or a fibre coil) that implements the constant differential time delay between the filter samples.

The feasibility of this approach has been experimentally demonstrated with a six-sample uniform RF photonic filter with three positive and three negative coefficients using the laser array implementation described in [84]. Figure 24 shows the experimental layout. An array of six tuneable lasers emitting at $\lambda_1 = 1546.65$ nm, $\lambda_2 = 1548.43$ nm, $\lambda_3 = 1550.11$ nm, $\lambda_4 = 1551.86$ nm, $\lambda_5 = 1553.47$ nm, and $\lambda_6 = 1555.24$ nm was selectively fed to two MZ modulators biased at $V^{+}_{BIAS} = 0$ V and $V^{-}_{BIAS} = -3.9$ V, respectively. Wavelengths λ_1, λ_3 and λ_5 were fed to the MZM biased at V^{+}_{BIAS} (positive samples), whereas wavelengths λ_2, λ_4 and λ_6 were fed to the MZM biased at V^{-}_{BIAS} (negative samples). Both EOM were modulated by the same RF signal, a 5 dBm sinusoidal signal provided by an optical component analyser (OCA). The frequency of the RF modulating signal was varied from 130 MHz to 5 GHz to measure the transfer function characteristic of the filter.

Figure 25 shows the measured modulus of the transfer function for a filter with six uniform coefficients. Both the experimental (solid line) and the theoretical (broken line) results are shown for reference and comparison. As

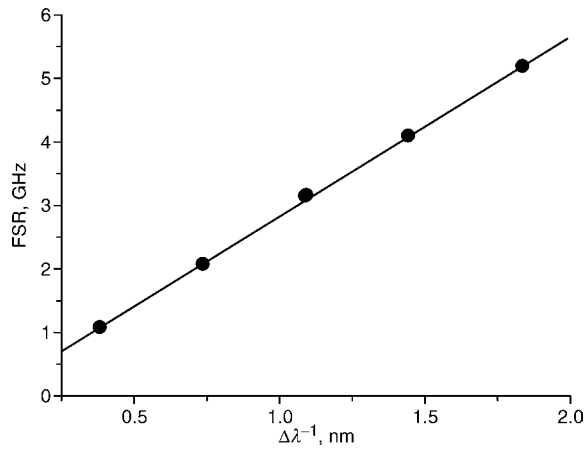

Fig. 22 *Free spectral range of the RF filters dependence on the reciprocal of the wavelength spacing between taps*
Theoretical calculation (solid line) and experimental results (dots)

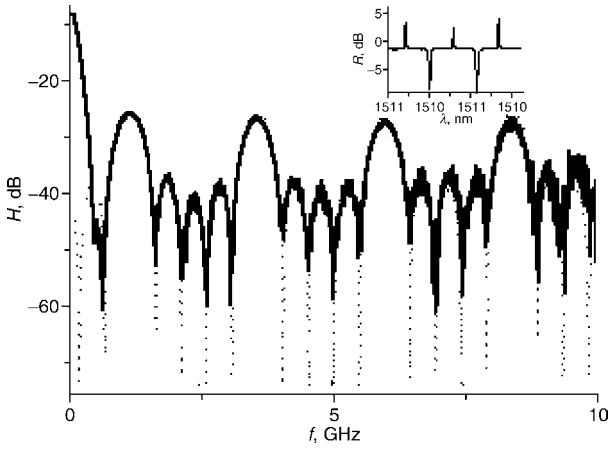

Fig. 23 *Filter response against RF signal frequency with 1.16 nm-equispaced*
Theoretical calculation (dotted line) and experimental results (solid line). Inset: Spectral position of the 5-taps

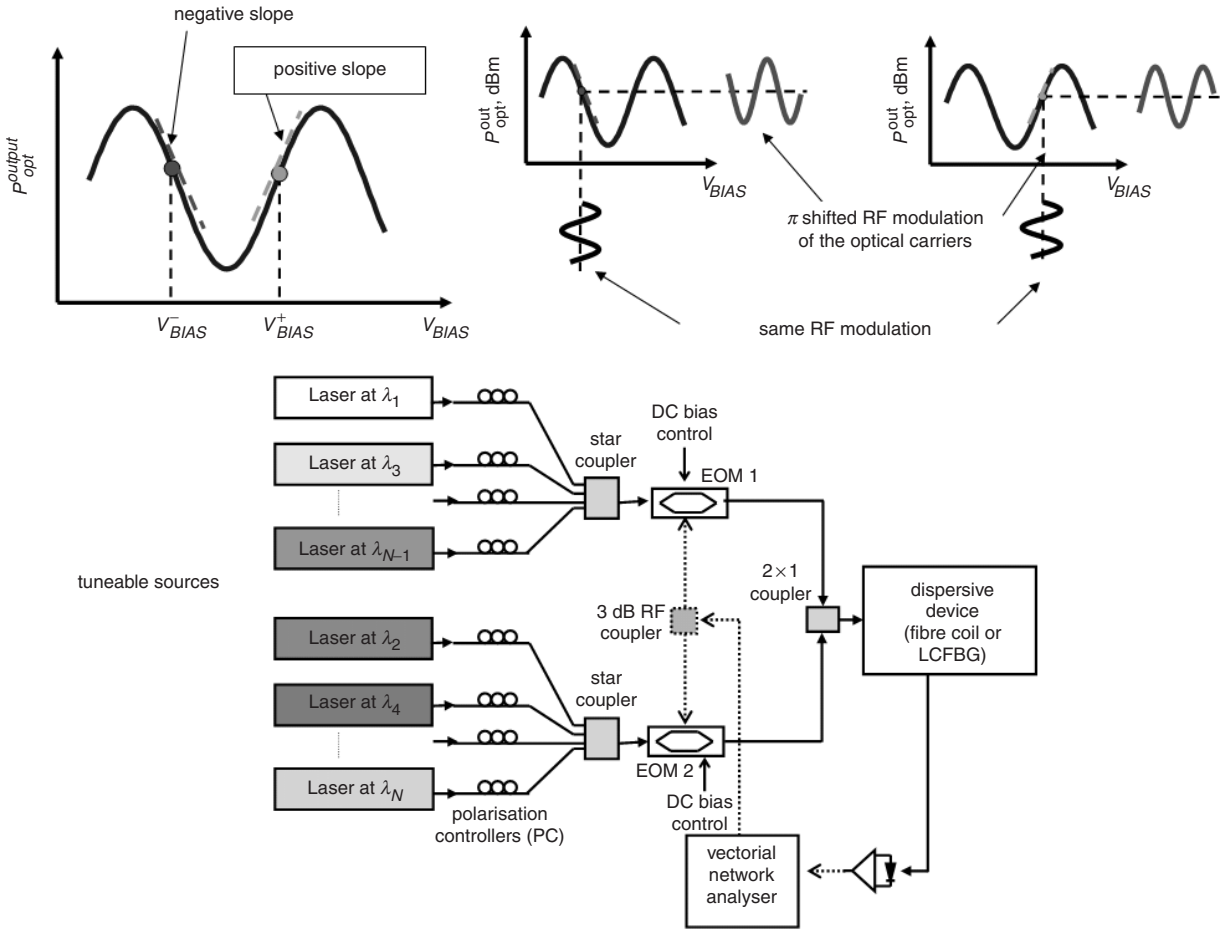

Fig. 24 *Experimental layout of the negative coefficient approach*
Employing two EOMs and counter phase modulation details at different biasing points of the EOM response

expected, the filter resonance at baseband (typical of positive coefficient filters) has been eliminated thus confirming the feasibility of the proposed scheme for the implementation of negative coefficients. Although in principle as shown in Fig. 25 two modulators are required in the transmitter in practice this requirement can be reduced to only one modulator if this device is provided with two input ports. A main advantage of this configuration is that there is no need to duplicate the optical structure of the filter to implement positive and negative coefficients since the taps already carry their sign prior to be delayed. Another interesting feature is that the sign is decoupled from any sample weighting process.

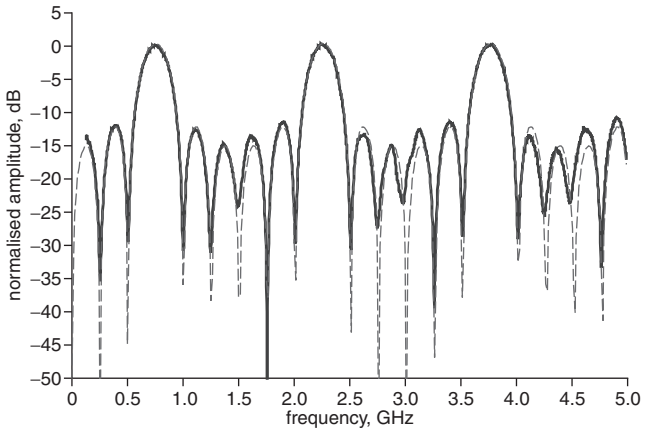

Fig. 25 *Measured modulus of the transfer function for a filter with six uniform coefficients*
Experimental (solid line) and the theoretical (broken line)

We mentioned in the preceeding paragraph that only a MZM device would be required if it has two inputs. This is achieved in practice by replacing the input *Y* branch to the integrated modulator by a 2×2 integrated coupler. We have reported novel results [85] using a newly developed 2×1 MZM device fabricated by AMS (Alenia Marconi Systems) featuring the above desired characteristics. We demonstrate a filter structure that requires only this device and we employ it to implement a nine-tap (positive and negative) transversal RF photonic reconfigurable filter with square-type resonances.

Figure 26 shows the layout and the intensity transfer function of the newly developed device. The device is a $LiNbO_3$ dual drive MZ modulator developed for this application within the framework of the EU funded IST-LABELS project. As it can be observed, the input *Y* branch has been replaced by a 3 dB 2×2 integrated coupler. Figure 26 also shows the measured modulation curves for the two (input 1-output) (input 2-output) input/output configurations. As expected, the curves for the two input/output configurations show a clear 180° phase shift on the two RF modulated outputs with maximum dynamic range at the quadrature point. Note as well that the 180° phase shift on the two RF modulated outputs is maintained regardless of the value of the bias voltage even if the output average power changes. For instance, the Figure shows two cases ((i) and (ii)) as particular examples. It must be pointed out however that working far from the quadrature bias

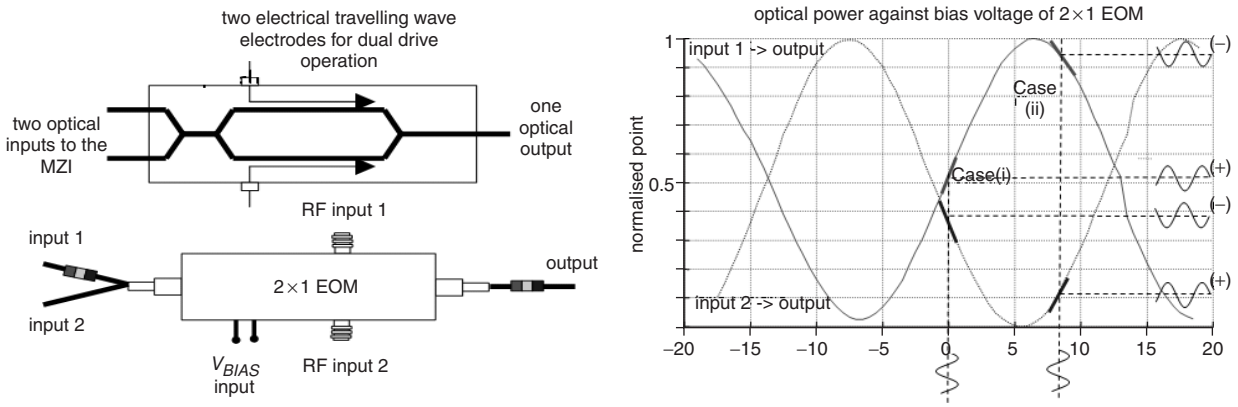

Fig. 26 *Layout and the intensity transfer function of the newly developed device*

voltage will generate considerable second-order distorsion that will compromise the linear behaviour of the filter. The 2 × 1 MZM previously described has been employed to demonstrate the operation concept in an experiment designed to implement, for the first time to our knowledge, a reconfigurable square type filter with negative coefficients. The filter layout was similar to that of Fig. 24 [85] with the exception that the two standard MZM modulators have been replaced by the especially designed 2 × 1 MZM. In this case the dispersive element was implemented by a 23 km and the filter samples were produced by means of tuneable lasers with wavelength separation of 0.96 nm between adjacent carriers that results in a filter-free spectral range of 2.63 GHz. The implemented RF filter was a square shape type with nine coefficients, (7 different from 0+2 null ones), with four negative taps. The values for the taps were [−0.16 0 0.27, −0.77 1 −0.77 0.27 0 −0.16]. Figure 27*a* shows the optical spectrum at the fibre coil output prior to the detector, and the measured transfer function (dotted trace), the theoretical expected trace for the square filter design (continuous trace) and also the theoretical trace for a filter with uniform coefficients (broken trace), in Fig. 27*b*. The agreement between the theoretical and the experimental results is excellent inside the filter bandpass. Outside the filter bandpass the agreement is worse, but this is due mainly to the noise arising from delay nonuniformities due to inaccuracies in the central wavelengths of the lasers and also due to the foreseeable inaccuracy in the tap amplitude.

3.2 *Transversal filters based on tuneable dispersive devices*

Chirped fibre Bragg gratings (CFBGs) have been proposed to obtain tuneable dispersion slope gratings showing suitable optical bandwidth for RF applications. By acting on them, it is possible to vary the time delay of each optical wavelength carrier. Temperature and strain gradients on the CFBG or the use of piezoelectric transducer are some of the most extended approaches. Recently, we demonstrated the possibility of generating a controllable chirp in a uniform fibre Bragg grating by fixing the device to a magnetostrictive rod, which could be disturbed with a tapered magnetic circuit. These magnetic systems show advantages such as good dynamic response and easy implementation.

A new device based on tuning the phase response of a tapered fibre Bragg grating (TFBG) by using a magnetostrictive transducer and the magnetic field inside a simple coil. Tuneable transversal filters can be implemented by using this device since the dispersion slope is tuned when applied current to the coil is varied.

The tuneable dispersion device consists of a chirped grating with tapered transversal section held on a magnetostrictive material, which is subjected to the nonuniform magnetic field produced by the current flow through a finite solenoid.

A 5 cm-long FBG with uniform period is written in a tapered fibre fabricated by fusion and elongation [86]. This TFBG is fixed on a magnetostrictive rod and placed inside of a 4 cm-long magnetic coil (see Fig. 28). Thus, the magnetostrictive material suffers a local lengthening, which is proportional to the intensity of the applied magnetic field. The TFBG is located at the axial region where the magnetic field variation is quasilinear [65]. Therefore, when an electrical current of a given intensity is injected to the solenoid, the magnetic field applied to the TFBG leads to different dispersion slopes depending on the intensity current. When no current is applied, the TFBG has a linear dispersion due to the design of the taper profile [86]. It has a flat reflectivity and a 3 dB bandwidth of 1.58 nm. The inset of Fig. 28 shows the dispersion slope when electric currents are 0, 3 and 5 A, with a 3 dB bandwidth of 1.58, 2.05 and 2.51 nm, respectively. Time

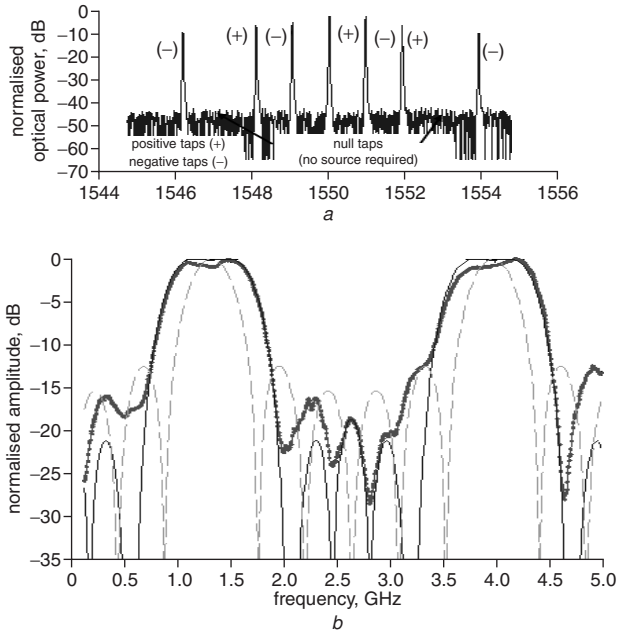

Fig. 27 *Optical spectrum and transfer functions*

a Optical spectrum of the detector, 9 taps (7 active and 2 null taps)
b Measured transfer function (dotted trace), the theoretical expected trace (continuous trace) and the theoretical trace for a filter with uniform coefficients (broken trace)

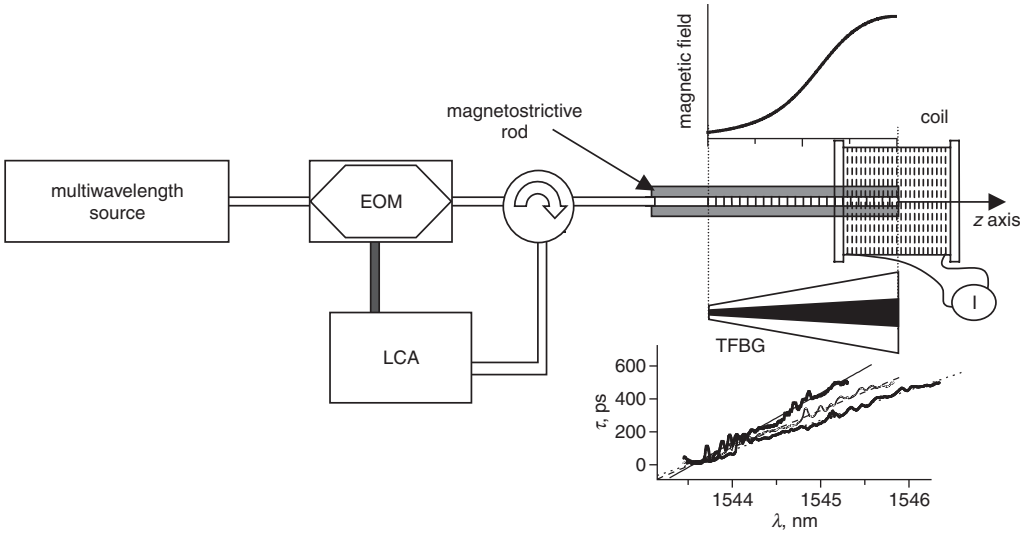

Fig. 28 *Tuneable device for RF filtering implementation based on fibre Bragg gratings subjected to nonuniform magnetic fields*
Inset: Time delay response when different electrical currents are applied: 1 = 0 (solid line), 3 (dashed line) and 5 A (dotted line)

delay slopes are achieved from 188 to 472 ps/nm, with a useful passband larger than 1 nm.

The implementation of RF filters requires N optical carriers, equidistant by $\Delta\lambda_0/(N-1)$, which are provided by a multiwavelength tuneable laser. They are amplitude modulated by an electro-optical modulator (EOM) and launched into the tuneable TFBG as shown in Fig. 28 [86]. The dispersion of the TFBG, D, gives the differential delay between adjacent optical taps. Because of the variation of the time delay slope of the TFBG when we apply different magnetic gradients, transversal notch filters with tuneable free spectral range (FSR) are measured.

Figure 29 shows the range of FSR values that can be obtained by using our device (shaded region). Moreover, several filters have been implemented by changing the number of optical taps and the total optical bandwidth $\Delta\lambda_0$ of the filter for 0, 5 and −5 amp. The inset shows an RF filter with $\Delta\lambda_0 = 1.0$ nm and two taps when $I = -5$ A ($D = 188$ ps/nm) and $I = 5$ A ($D = 472$ ps/nm) showing a FSR of 5.4 and 2.3 GHz, respectively.

The tuning range of the previous approach can be enlarged by using a new system composed of the cascade of two switched tuneable stages [65]. Each one includes a tapered fibre grating subjected to the nonuniform magnetic field created inside an electrical coil. Figure 30 shows a scheme of this tuneable dispersion system. A laser source is amplitude modulated and launched into the first TFBG through a circulator. The optical signal reflected goes through a 50–50 coupler, and then, to an optical switch. When it is in the bar state (BS) the optical signal is launched into the second TFBG, and therefore, the response of the global system is given by the cascade of both subsystems. After reflection in the second grating, the signal is measured at one of the input ports of the coupler by using a lightwave components analyser. Alternatively, when the optical switch is in the cross state (CS), the signal is driven to the LCA through the output port of the switch.

Measurements of the amplitude and time delay response of the whole system were performed with the optical switch in CS and BS. First state led to dispersion slopes from 230 to 351 ps/nm, whereas a range between 420 and 715 ps/nm was obtained in the second state. To show the performance of this system, three-taps RF filters were implemented for CS and BS when different electrical currents are injected to the solenoid (0, 2 and 4 A). The multiwavelength was set to emit light at three different optical wavelengths equispaced by 0.41 nm. Figure 31 shows the FSR of the measured RF filters for different electrical currents. CS led to achieve FSRs between 7 and 10.6 GHz and BS led to a tuning range from 3.5 to 5.8 GHz. The inset of Fig. 31 shows the group time delay against wavelength when no electrical current is applied to the coils. Note the increase of the dispersion when BS was set instead of CS.

Amongst the approaches based on keeping fixed the wavelengths implementing the filter taps and changing the dispersion of the delay line to obtain variable filter basic delays and therefore to provide RF bandpass tuning, we can include the following RF photonic filter, although in this case other important techniques as spectral slicing employing uniform FBGs and fibre delay lines have been combined to perform the filter specifications. More specifically, within the EU funded IST LABELS project we have developed a tuneable photonic filter for noise suppression and channel interference mitigation in the front-end stage of an UMTS base station prior to the highly selective SAW filter. As it has been reported elsewhere [9], the inclusion of such a filter can increase

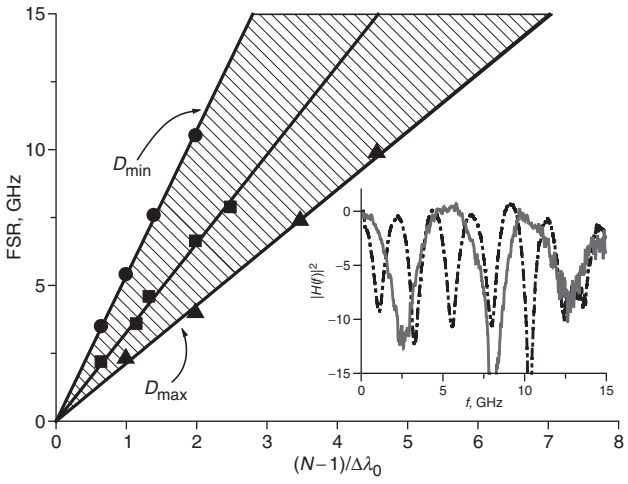

Fig. 29 *FSR against number of optical taps and optical bandwidth of the filter for different time delay slopes*
Inset: Transfer function of a tuned RF filter (solid line: $D = 188$ ps/nm, dashed line: $D = 472$ ps/nm)

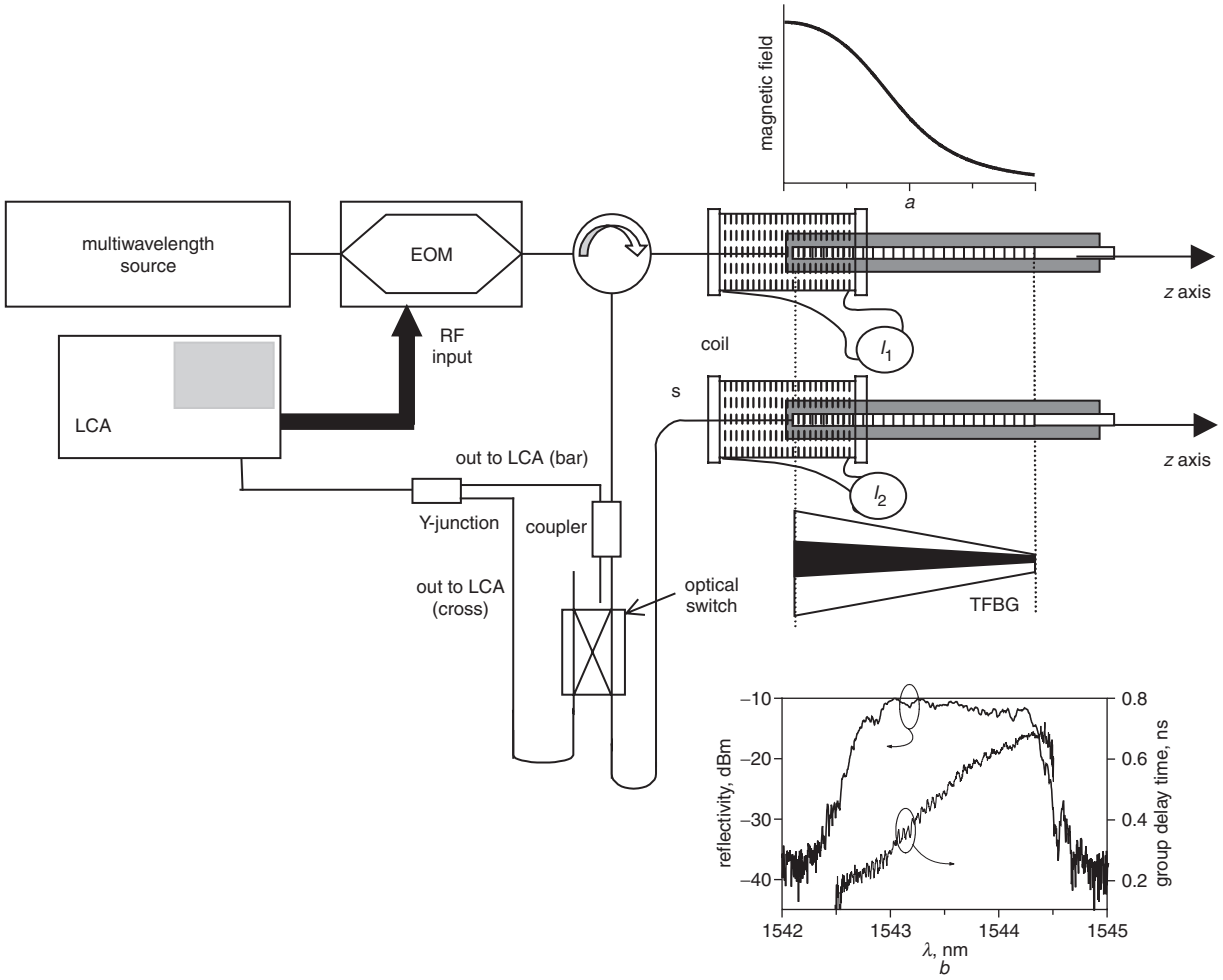

Fig. 30 *Schematic of the optically switched time delay line*

Insets:
a Dependence of the magnetic field on the *z*-axis along the grating
b Reflectivity and time delay response of one of the chirped fibre gratings

the capacity of UMTS systems. The designed filter is able to be switched along the 12-channel UMTS.

The proposed configuration implements a classical FIR transversal filter. We also employ the spectral slicing of a high power broadband optical source to obtain an 'equivalent' multiwavelength source. The slicing is performed by an array of fibre Bragg gratings which also introduces a fixed time delay between the reflected slices of the signal. Finally, we employ a reconfigurable chain of dispersive modules (SMF-28 fibre) to vary the time-delay between the slices and thus introduce tuneability to the filter. Figure 32 shows the filter structure. The first block is the optical source and modulator, where a super light-emitting diode (SLED) is employed as the broadband optical source (power of 10 mW and with the 40 nm bandwidth at 1555 nm). The RF modulation of the optical signal is performed by means of a MZ electro-optical modulator (EOM) directly over the entire SLED spectrum. The second block consists of an array of N fibre Bragg gratings written in series with certain uniform spacing between the gratings. This block accomplishes a double task: the slicing of the SLED spectrum and the introduction of the time delay between the signals reflected from the gratings. Finally, the spectral slices are fed to the third block: a reconfigurable chain of dispersive modules, where each module employs a standard nonshifted SMF-28 fibre (the use of a highly dispersive, e.g. a dispersion compensating fibre, is also possible). The optical switches in the third block provide a stepwise tuning of the accumulated dispersion in the block. By varying the dispersion of the block, the time delay between the signals reflected from different gratings is changed and thus, tuneability of the filter RF response is achieved.

The UMTS channel filtering requires a high Q factor (about 400), since the required 3 dB pass-band of the filter

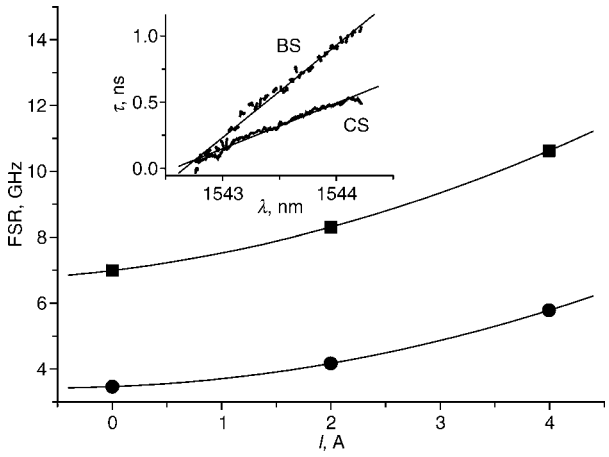

Fig. 31 *Free spectral range of the RF filters against the current intensity*

For cross (■) and bar (●) states of the switch. Inset: Group delay time for cross state (351 ps/nm; solid line) and bar state (712 ps/nm; dotted line) when no current is applied to the solenoids

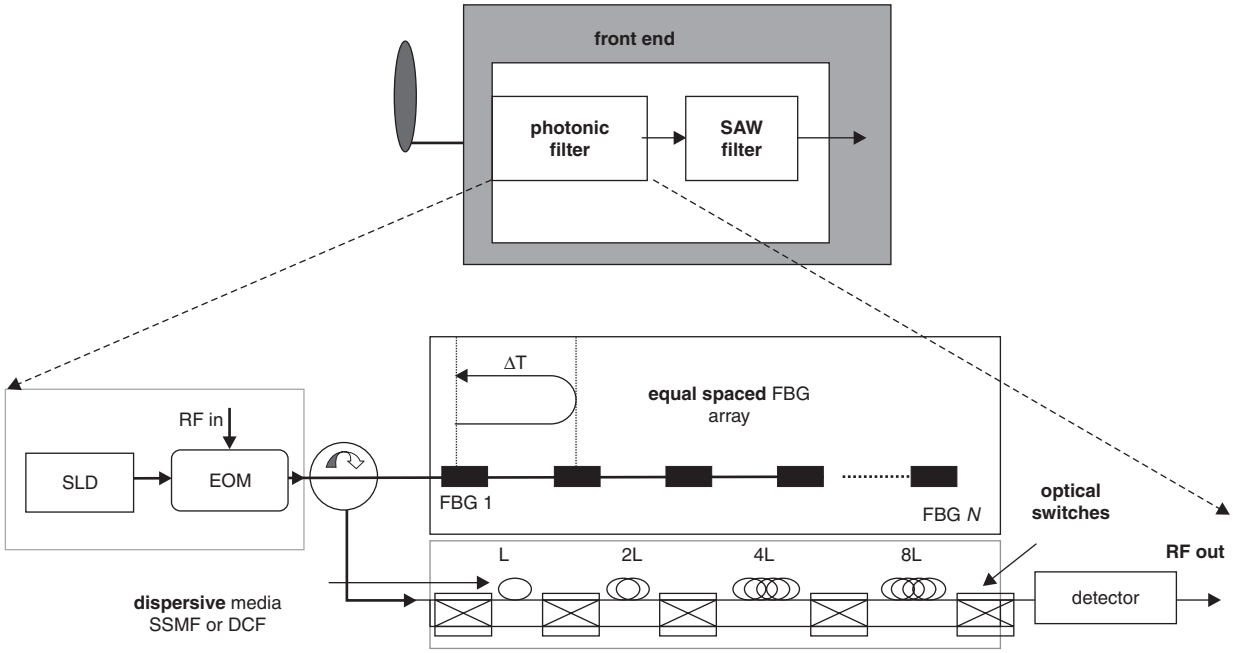

Fig. 32 *UMTS photonic filter set up*

should be less than 5 MHz and the operating frequency of the filter lies within 1920–1980 MHz. Furthermore, the UMTS channel filtering also requires the tuneability of the RF pass-band within the 12 channels allocated along the 60 MHz band (between 1920 and 1980 MHz). To achieve such a high Q-factor, the present transversal filter operates at a higher order 'resonance' of its periodic response. In this case, the FSR of the filter is an integer fraction of the UMTS operating frequency. The present filter has been designed to employ the resonance number 18. To keep the filter tuned to the upper UMTS channel at 1977 MHz when the dispersive module is 'switched off', the FSR of the filter has been set to 109 MHz, and the corresponding spacing between the adjacent gratings has been set to 930 mm. The other design parameters are the total number of gratings N and the gratings reflectivity as a function of wavelength or grating number. The goal in the filter design was to achieve a 3 dB bandwidth within 5–6 MHz, a 1 dB bandwidth larger than 3 MHz, and the side-lobe rejection level larger than 40 dB. In order to meet the above rejection level, a normalised Gaussian apodisation of the taps weights has been employed. The total number of required gratings has been determined from the indicated above target bandwidth being finally fixed to $N = 30$. The last filter parameter to be determined was the FBG wavelength spacing that was set to 1 nm which ensured that the SLED optical spectrum (40 nm) was used efficiently. The 1-nm spacing has also established the length of the SMF-28 fibre required for proper switching of the operating frequency between the UMTS channels. We determined that 5 MHz steps towards lower RF frequencies require an increase of 23 ps in the time delay which corresponds to about 1.35 km of SMF-28 fibre with the dispersion of 17 ps/(nm km) at 1550 nm.

The fabricated gratings have been made 1 cm long, Hamming apodised and had the 3 dB bandwidth about 44 pm. Each grating has been fabricated separately and then the gratings have been spliced to each other with the 930 mm centre-to-centre spacing. Figures 33*a* and *b* show the view over the 17–19th and over the 18th resonance of the filter response. Each of the eight traces in either Figure corresponds to a different amount of dispersion provided by the reconfigurable dispersive module. The introduced optical insertion loss of 7 dB due to the 10.7-km long fibre and connectors (2 dB from the fibre and 5 dB from the connectors) has been compensated in the experiment by an adjustable EDFA prior to the detector. One can see that the operation frequency of the filter varies

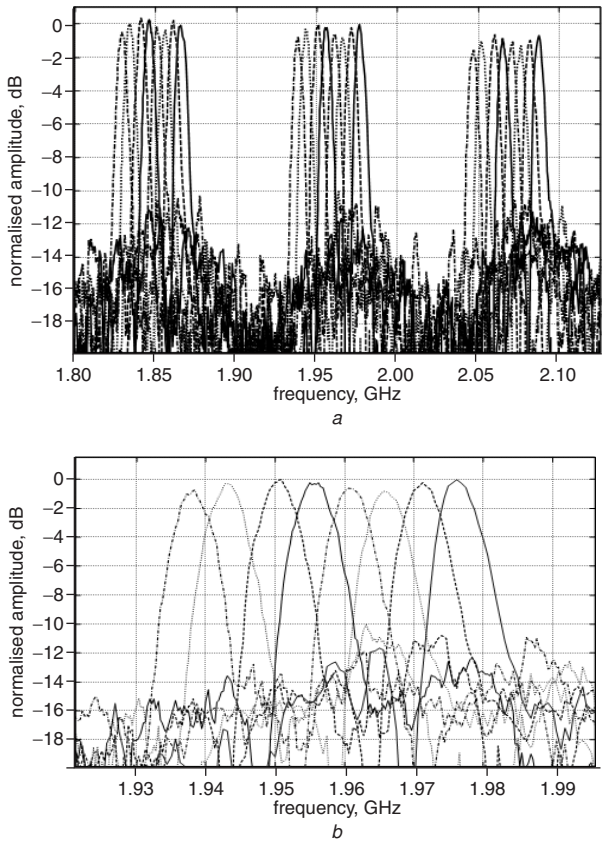

Fig. 33 *UMTS filter response*

a 17–19th
b Detail over the 18th resonance
Each of the 8 traces in either figure corresponds to a different amount of dispersion provided by the reconfigurable dispersive module in different steps from 0 km (higher frequency trace) up to 10.7 km (lower frequency trace)

almost linearly against the standard fibre length with the slope of 3.577 MHz/km (i.e. 1.39 km less or extra fibre is required for the shift of 5 MHz). The rejection levels have been obtained for each tuning position by measuring the range from the main lobe to the highest sidelobe level inside the rejected band, giving the 12, 13.4, 13.4, 12.8, 13, 11.4, 10.9, and 10.9 dB, respectively. The small RL is mainly due to the spacing errors between the gratings, which we can also conclude from the fact that the rejection level, RL, is frequency dependent (e.g. the measurements give RL $>$ 24 dB at 500 MHz).

4 Current challenges, summary and conclusions

It should be clear from what it has been stated so far that the main challenges that researchers have to face in this area are to:

(*a*) Develop technology options that allow tuneable filters over a wide region of spectral bands of present and future RF applications.
(*b*) Obtain architectures featuring filter reconfigurability by means of external control signals.
(*c*) Obtain high Q filters.

Much progress has been achieved in items (*a*) and (*b*), some of which have been developed by our group and have been presented in this paper. Significant contributions from other research groups can also be found in the literature. The last item, i.e. the obtention of high Q filters has been scarcely addressed in the literature so far. Yet it is essential to develop techniques leading to microwave photonic filters with Q factors comparable to other competing options.

In this paper, we have presented the most recent advances in the implementation of photonic tuneable transversal filters for RF signal processing developed by our group. After a brief introduction to the field and the basic concepts, limiting factors and application of these filters we have described our work in the field. To do so, we have classified the group of tuneable filters into two groups. The first is composed of those based on wavelength tuneable optical taps. The second group include those filters where the bandpass tuneability is achieved by changing the dispersion of the optical delay lines to provide the variable time delay between samples.

On one hand, interesting results related to the large degree of flexibility shown by the tuneable laser array and chirped grating based structure have been shown together with other cheaper alternatives based on the slicing of broadband optical sources either by using tuneable fibre Bragg gratings or by using arrayed waveguide gratings. Other alternatives to implement flexible and low-cost tuneable transversal filters based on the generation of multiple taps by using an acousto-optic modulation on the fibre Bragg grating.

Also, structures featuring high perfomance filters such as the bandpass filter implemented by using a Mach-Zehnder interferometer and a broadband optical source, or the implementation of filters with negative coefficients have been discussed. These filters have been recently demonstrated by using two different approaches, which are also described in this paper. Either by setting different bias voltage in an electro-optic modulator or by using fibre Bragg gratings in transmission, larger flexibility in the filter response given by the implementation of negative coefficients is demonstrated.

On the other hand, proposals on tuneable dispersive devices based on the tuneability of the chirped fibre Bragg gratings characteristics have also been addressed in a single stage or in a cascade by means of using an optical switch to increase the tuneability range of these structures. Finally, a 30-taps transversal filter implemented by using a broadband optical source sliced by 30 uniform fibre gratings is designed for selecting channels in an UMTS application. In this structure, the physical spacing between the gratings provide the initial response and the filter tuneability is achieved by means of a series of different switched fibre delay lines.

5 Acknowledgments

The authors wish to acknowledge the EU funded research projects IST-2001-37435 (LABELS) and IST-2001-32786 (NEFERTITI) and the MCYT support through the Ayudas a Parques Científicos and Infrestructuras FEDER programmes and project TIC2002-04344 PROFECIA under which part of the work reported here is being carried.

6 References

1 Seeds, A.: 'Microwave photonics', *IEEE Trans. Microw. Theory Tech.*, 2002, **50**, pp. 877–887
2 Jackson, K., Newton, S., Moslehi, B., Tur, M., Cutler, C., Goodman, J., and Shaw, H.J.: 'Optical fibre delay-line signal processing', *IEEE Trans. Microw. Theory Tech.*, 1985, **33**, pp. 193–204
3 Wilner, K., and Van Den Heuvel, A.P.: 'Fibre-optic delay lines for microwave signal processing', *Proc. IEEE*, 1976, **64**, pp. 805–807
4 Chang, C., Cassaboom, J.A., and Taylor, H.F.: 'Fibre optic delay line devices for RF signal processing', *Electron. Lett.*, 1977, **13**, pp. 678–680
5 Taylor, H.F.: 'Fibre and integrated optical devices for signal processing', *SPIE*, 1979, **176**, pp. 17–27
6 Jackson, K.P., and Shaw, H.J.: 'Fibre-optic delay-line signal processors' *in* 'Optical signal processing' (Academic Press, San Diego, 1987), chap. 7
7 Minasian, R.A., Alameh, K.E., and Chan, E.H.W.: 'Photonics-based interference mitigation filters', *IEEE Trans. Microw. Theory Tech.*, 2001, **49**, pp. 1894–1899
8 Pastor, D., Ortega, B., Capmany, J., Fonjallaz, P.-Y., and Popov, M.: 'Tunable microwave photonic filter for noise and interference suppression in UMTS base stations', *Electron. Lett.*, 2004, **40**, pp. 997–999
9 Kitayama, K.I.: 'Architectural considerations of fibre-radio millimeter-wave wireless access systems', *J. Fib. Integ. Opt.*, 2000, **19**, pp. 167–186
10 Sugiyama, T., Suzuki, M., and Kubota, S.: 'An integrated interference suppression scheme with adaptative equalizer for digital satellite communication systems', *IEICE Trans. Commun.*, 1996, **E79-B**, pp. 191–196
11 Skolnik, M.I.: 'Introduction to radar systems' (McGraw-Hill, 1980)
12 See for instance Blumenthal, D.J., *et al.*: 'All-optical label swapping networks and technologies', *JLT*, 2000, **18**, (12), pp. 2058–2075 and A. Carena, *et al.*, 'OPERA: An optical packet experimental routing architecture with label swapping capability', *JLT*, 1998, **16**, (12), pp. 2135–2145
13 Capmany, J., Ortega, B., Martinez, A., Pastor, D., Popov, M., and Fonjallaz, P.-Y.: 'Multi-wavelength single sideband modulation for WDM radio over fibre systems using a fibre grating array tandem device', *IEEE Photonics Technol. Lett.*, 2005, **17**, pp. 471–473
14 Moslehi, B.: 'Fibre-optic filters employing optical amplifiers to provide design flexibility', *Electron. Lett.*, 1992, **28**, pp. 226–228
15 Capmany, J., and Cascón, J.: 'Optical programmable transversal filters using fibre amplifiers', *Electron. Lett.*, 1992, **28**, pp. 1245–1246
16 Polo, V., Ramos, F., Martí, J., Wake, D., and Moodie, D.: 'Synthesis of photonic microwave filters based on external optical modulators and wide-band chirped fibre gratings', *IEEE J. Lightwave Technol.*, 2000, **18**, pp. 213–220
17 Moslehi, B., Chau, K., and Goodman, J.W.: 'Optical amplifiers and liquid-crystal shutters applied to electrically reconfigurable fibre optic signal processors', *Opt. Eng.*, 1993, **32**, pp. 974–981
18 Capmany, J., and Cascón, J.: 'Direct form I fibre-optic discrete-time signal processors using optical amplifiers and embedded Mach-Zehnder structures', *IEEE Photonics Technol. Lett.*, 1993, **5**, pp. 842–844
19 Pastor, D., Sales, S., Capmany, J., Martí, J., and Cascón, J.: 'Amplified double-coupler fibre-optic delay line filter', *IEEE Photonics Technol. Lett.*, 1995, **7**, pp. 75–77

20 Capmany, J., Cascón, J., Marín, J.L., and Martí, J.: 'Fibre-optic delay line filter synthesis employing a modified PADE method', *Electron. Lett.*, 1995, **31**, pp. 479–480
21 Sales, S., Capmany, J., Martí, J., and Pastor, D.: 'Experimental demonstration of fibre-optic delay line filters with negative coefficients', *Electron. Lett.*, 1995, **31**, pp. 1095–1096
22 Sales, S., Capmany, J., Pastor, D., and Martí, J.: 'Fibre-optic delay line filters employing fibre loops: Signal and noise analysis and experimental characterization', *J. Opt. Soc. Am. A, JOSA A*, 1995, pp. 2129–2135
23 Capmany, J., Cascón, J., Marín, J.L., Sales, S., Pastor, D., and Martí, J.: 'Synthesis of fibre-optic delay line filters', *IEEE J. Lightwave Technol.*, 1995, **13**, pp. 2003–2012
24 Heyde, E., and Minasian, R.A.: 'A solution to the synthesis problem of recirculating delay line filters', *IEEE Photonics Technol. Lett.*, 1995, **6**, pp. 833–835
25 Sales, S., Capmany, J., Martí, J., and Pastor, D.: 'Novel and significant results on the nonrecirculating delay line with a fibre loop', *IEEE Photonics Technol. Lett.*, 1995, **6**, pp. 1439–1440
26 Norton, D., Johns, S., Keefer, C., and Soref, R.: 'Tunable microwave filtering using high dispersion fibre time delays', *IEEE Photonics Technol. Lett.*, 1994, **6**, pp. 831–832
27 Frankel, M.Y., and Esman, R.D.: 'Fibre-optic transversal filter', *IEEE Photonics Technol. Lett.*, 1995, **7**, pp. 191–193
28 Yegnanarayanan, S., Trinh, P.D., and Jalali, B.: 'Recirculating photonic filter: a wavelength-selective time delay for phased-array antennas and wavelength code-division multiple access', *Opt. Lett.*, 1996, **21**, pp. 740–742
29 Coppinger, F., *et al*.: 'Nonrecursive photonic filter using wavelength-selective true time dely', *IEEE Photonics Technol. Lett.*, 1996, **8**, pp. 1214–1216
30 Coppinger, F., *et al*.: 'Continuously tunable photonic radio-frequency notch filter', *IEEE Photonics Technol. Lett.*, 1997, **9**, pp. 339–341
31 You, N., and Minasian, R.A.: 'A novel tunable microwave optical notch filter', *IEEE Trans. Microw. Theory Tech.*, 2001, **49**, pp. 2002–2005
32 Foord, A.P., and Davies Greenhalgh, P.A.: 'Synthesis of microwave and millimetre-wave filters using optical spectrum-slicing', *Electron. Lett.*, 1996, **32**, pp. 390–391
33 Capmany, J., Pastor, D., and Ortega, B.: 'Fibre-optic microwave and millimetre wave filter with high density sampling and very high sidelobe suppression using subnanometre optical spectrum slicing', *Electron. Lett.*, 1999, **35**, pp. 494–496
34 Pastor, D., Capmany, J., and Ortega, B.: 'Broad-band tunable microwave transversal notch filter based on tunable uniform fibre Bragg gratings as slicing filters', *IEEE Photonics Technol. Lett.*, 2001, **13**, pp. 726–728
35 Mora, J., Ortega, B., Capmany, J., Cruz, J.L., Andres, M.V., Pastor, D., and Sales, S.: 'Automatic tunable and reconfigurable fibre-optic microwave filters based on a broadband optical source sliced by uniform fibre Bragg gratings', *Opt. Express*, **10**, 2002, pp. 1291–1298
36 Yegnanarayanan, S., *et al*.: 'Microwave transversal filter based on spectral tapping of broadband light in an integrated waveguide prism', P CWF55 Proc. CLEO '97, 1997, p. 259
37 Pastor, D., Ortega, B., Capmany, J., Sales, S., and Muñoz, P.: 'Flexible and tunable microwave filters based on arrayed waveguide gratings'. Proc. IEEE Topical Meeting on Microwave Photonics, 2002, pp. 189–192
38 Yost, T., Herczfeld, P., Rosen, A., and Singh, S.: 'Hybrid transversal filter utilizing MMIC and optical fibre delay lines', *IEEE Microw. Guided Wave Lett.*, 1995, **5**, pp. 287–289
39 Zhang, W., and Williams, J.A.R.: 'Fibre optic bandpass transversal filter employing fibre grating arrays', *Electron. Lett.*, 1999, **35**, pp. 1010–1011
40 Pastor, D., Capmany, J., Sales, S., Muñoz, P., and Ortega, B.: 'Reconfigurable fibre-optic-based RF filters using current injection in multimode lasers', *IEEE Photonics Technol. Lett.*, 2001, **13**, pp. 1224–1226
41 Ball, G.A., Glenn, W.H., and Morey, W.W.: 'Programmable fibre optic delay line', *IEEE Photonics Technol. Lett.*, 1994, **6**, pp. 741–743
42 Hunter, D.B., and Minasian, R.A.: 'Tunable transversal filter based on chirped gratings', *Electron. Lett.*, 1995, **31**, pp. 2205–2207
43 Hunter, D.B., and Minasian, R.A.: 'Microwave optical filters using in-fibre Bragg grating arrays', *IEEE Microw. Guided Wave Lett.*, 1996, **6**, pp. 103–105
44 Zhang, W., and Williams, J.A.R.: 'Fibre optic bandpass transversal filter employing fibre grating arrays', *Electron. Lett.*, 1999, **35**, pp. 1010–1011
45 Yu, G., Zhang, W., and Williams, J.A.R.: 'High-performance microwave transversal filter using fibre Bragg grating arrays', *IEEE Photonics Technol. Lett.*, 2000, **12**, pp. 1183–1185
46 Zhang, W., Williams, J.A.R., and Bennion, I.: 'Polarization synthesized optical transversal filter employing high birefringence fibre gratings', *IEEE Photonics Technol. Lett.*, 2001, **13**, pp. 523–525
47 Zhang, W., Yu, G., and Williams, J.A.R.: 'Tap multiplexed fibre grating-based optical tranversal filter', *Electron. Lett.*, 2000, **36**, pp. 1708–1710
48 Zhang, W., Williams, J.A.R., and Bennion, I.: 'Optical fibre recirculating delay line incorporating a fibre grating array', *IEEE Microw. Wireless Compon. Lett.*, 2001, **11**, pp. 217–219
49 Hunter, D.B., and Minasian, R.A.: 'Microwave optical filters based on a fibre Bragg grating in a loop structure'. Int. Topical Meeting on Microwave Photonics, MWP '96. Technical Digest, 1996, pp. 273–276
50 Hunter, D.B., and Minasian, R.A.: 'Photonic signal processing of microwave signals using active-fibre Bragg-grating-pair structure', *IEEE Trans. Microw. Theory Technol.*, 1997, **8**, pp. 1463–1466
51 You, N., and Minasian, R.A.: 'A novel high-Q optical microwave processor using hybrid delay line filters', *IEEE Trans. Microw. Theory Tech.*, 1999, **47**, pp. 1304–1308
52 Minasian, R.A., Alameh, K.E., and Chan, E.H.W.: 'Photonics-based interference mitigation filters', *IEEE Trans. Microw. Theory Tech.*, 2001, **49**, pp. 1894–1899
53 Chan, E.H.W., Alameh, K.E., and Minasian, R.A.: 'Photonic bandpass filter with high skirt selectivity and stopband attenuation', *IEEE J. Lightwave Technol.*, 2002, **20**, pp. 1962–1967
54 Zhang, W., Williams, J.A.R., Everall, L.A., and Bennion, I.: 'Fibre-optic radio frequency notch filter with linear and continuous tuning by using a chirped fibre grating', *Electron. Lett.*, 1998, **34**, pp. 1770–1772
55 Hunter, D.B., and Minasian, R.A.: 'Tunable microwave fibre-optic bandpass filters', *IEEE Photonics Technol. Lett.*, 1999, **11**, pp. 874–876
56 Pastor, D., and Capmany, J.: 'Fibre optic tunable transversal filter using laser array and linearly chirped fibre grating', *Electron. Lett.*, 1998, **34**, pp. 1684–1685
57 Capmany, J., Pastor, D., and Ortega, B.: 'Experimental demonstration of tuneability and transfer function reconfiguration in fibre-optic microwave filters composed of a linearly chirped fibre grating fed by a laser array', *Electron. Lett.*, 1998, **34**, pp. 2262–2264
58 Capmany, J., Pastor, D., and Ortega, B.: 'New and flexible fibre-optic delay line filters using chirped Bragg gratings and laser arrays', *IEEE Trans. Microw. Theory Tech.*, 1999, **47**, pp. 1321–1327
59 Pastor, D., Capmany, J., and Ortega, B.: 'Efficient sidelobe suppression by source power apodisation on fibre-optic microwave filters composed of linearly chirped fibre grating fed by laser array', *Electron. Lett.*, 1999, **35**, pp. 640–642
60 Pastor, D., Capmany, J., and Ortega, B.: 'Experimental demonstration of parallel fibre-optic-based RF filtering using WDM techniques', *IEEE Photonics Technol. Lett.*, 2000, **12**, pp. 77–79
61 You, N., and Minasian, R.A.: 'Synthesis of WDM grating-based optical microwave filter with arbitrary impulse response'. Int. Topical Meeting on Microwave Photonics, MWP '99, Vol. 1, 1999, pp. 223–226
62 Mora, J., Ortega, B., Andrés, M.V., Capmany, J., Cruz, J.L., Pastor, D., and Sales, S.: 'Dynamic optical transversal filters based on a tunable dispersion filter based on a tunable dispersion fibre Bragg grating'. Int. Topical Meeting on Microwave Photonics, MWP 2001, pp. 203–206
63 Oppenheim, A.V., Schaffer, R.W., and Buck, J.R.: 'Discrete time signal processing' (Prentice-Hall, Englewood Cliffs, 1996). See also Madsen, C., and Zhao, J.: 'Optical filter design: A signal processing approach' (John Wiley & Sons, New York, 1999)
64 Zhang, W., Williams, J.A.R., and Bennion, I.: 'Optical fibre delay line filter free of limitation imposed by optical coherence', *Electron. Lett.*, 1999, **35**, pp. 2133–2134
65 Mora, J., *et al*.: 'Highly tunable optically switched time delay line for transversal filtering', *Electron. Lett.*, 2003, **39**, (25), pp. 1799–1800
66 Vidal, B., Polo, V., Corral, J.L., and Martí, J.: 'Photonic microwave filter with tunning and reconfiguration capabilities using optical switches and dispersive media', *Electron. Lett.*, 2003, **39**, pp. 547–548
67 Pastor, D., *et al*.: 'Optical microwave filter based on spectral slicing by use of arrayed waveguide gratings', *Opt. Lett.*, 2003, **28**, (19), pp. 1802–1804
68 Ho-Quoc, A., Tedjini, S., and Hilt, A.: 'Optical polarization effect in discrete time fibre-optic structures for microwave signal processing', IEEE MTT-Symp. Digest, 1996, pp. 907–910
69 Coppinger, F., Yegnanarayanan, S., Trinh, P.D., and Jalali, B.: 'All-optical incoherent negative taps for photonic signal processing', *Electron. Lett.*, 1995, **33**, pp. 973–975

70 Tur, M., Moslehi, B., and Goodman, J.W.: 'Theory of laser phase noise in recirculating fibre optic delay lines', *IEEE J. Lightwave Technol.*, 1985, **3**, pp. 20–30
71 Tur, M., and Arie, A.: 'Phase induced intensity noise in concatenated fibre-optic delay lines', *IEEE J. Lightwave Technol.*, 1988, **6**, pp. 120–130
72 Moslehi, B.: 'Analysis of optical phase noise in fibre-optic systems employing a laser source with arbitrary coherence time', *IEEE J. Lightwave Technol.*, 1986, **4**, pp. 1334–1351
73 Kringlebotn, J.T., and Blotekjaer, K.: 'Noise analysis of an amplified fibre-optic recirculating delay line', *IEEE J. Lightwave Technol.*, 1994, **12**, pp. 573–581
74 Capmany, J.: 'Investigation on phase induced intensity noise in amplified fibre-optic recirculating delay line', *Electron. Lett.*, 1993, pp. 346–347
75 Hall, P.: 'The square kilometre array radio telescope'. Proc. Applicat. Radio Sci. Workshop, Apr. 2000, pp. 41–46
76 Pastor, D., *et al.*: 'Flexible and tunable microwave filters based on arrayed waveguide gratings'. Proc. IEEE Int. Topical Meeting on Microwave Photonics, 2002, pp. 189–192
77 Delgado-Pinar, M., Mora, J., Díez, A., Ortega, B., Andrés, M.V., and Capmany, J.: 'Tunable and reconfigurable microwave filter using a Bragg-grating based acoustooptic superlattice modulator', *Opt. Lett.*, 2005, **30**, pp. 8–10
78 Mora, J., Ortega, B., Andres, M.V., Capmany, J., Diez, A., and Pastor, D.: 'A single bandpass tunable photonic transversal filter based on a broadband optical source and a Mach-Zehnder interferometer', IEEE Int. Topical Meeting on Microwave Photonics, MWP, Budapest, Hungary, 2003, pp. 251–254
79 Coppinger, F., Yegnanarayanan, S., Trinh, P.D., and Jalali, B.: 'All-optical RF filter using amplitude inversion in a semiconductor optical amplifier', *IEEE Trans. Microw. Theory Tech.*, 1997, **45**, pp. 1473–1477
80 Shenping, Li, Chiang, K.S., Gambling, W.A., Liu, Y., Zhang, L., and Bennion, I.: 'A novel tunable all-optical incoherent negative-tap fibre-optic transversal filter based on a DFB laser diode and fibre bragg gratings', *IEEE Photonics Technol. Lett.*, 2000, **12**, pp. 1207–1209
81 Wang, X., and Chan, K.T.: 'Tunable all-optical incoherent bipolar delay-line using injection-locked Fabry-Perot laser and fibre Bragg gratings', *Electron. Lett.*, 2000, **36**, pp. 2001–2003
82 Xiaoke, Y., Fang, W., Jun Hong, N., and Chao, L.: 'Tunable microwave filters design using wavelength conversion technique and high dispersion time delays', *IEEE Photonics Technol. Lett.*, 2001, **13**, pp. 857–859
83 Mora, J., Ortega, B., Andrés, M.V., Capmany, J., Cruz, J.L., Pastor, D., and Sales, S.: 'Tunable all-optical negative multi-tap microwave filters based on uniform fibre Bragg gratings', *Opt. Lett.*, 2003, **28**, pp. 1038–1310
84 Capmany, J., Pastor, D., Martinez, A., Ortega, B., and Sales, S.: 'Microwave photonic filters with negative coefficients based on phase inversion in an electro-optic modulator', *Opt. Lett.*, 2003, **28**, pp. 1415–1417
85 Pastor, D., *et al.*: 'Reconfigurable RF photonic filter with negative coefficients and flat top resonances using phase inversion in a newly designed 2×1 integrated Mach-Zehnder modulator', *IEEE Photonics. Technol. Lett.* (accepted for publication)
86 Mora, J., Ortega, B., Andrés, M.V., Capmany, J., Cruz, J.L., Pastor, D., and Sales, S.: 'Tuneable dispersion device based on a tapered fibre Bragg grating and nonuniform magnetic fields', *IEEE Photonics Technol. Lett.*, 2003, **15**, pp. 951–953